GEOLOGICAL SURVEY OF CANADA

OPEN FILE 5182

Morphology, petrography, age and origin of the Fogo Seamounts, eastern Canada

G. Pe-Piper, A. de Jonge, D.J.W. Piper, L.F. Jansa

2006

Natural Resources Canada Ressources naturelles Canada

Canada

GEOLOGICAL SURVEY OF CANADA

OPEN FILE 5182

Morphology, petrography, age and origin of the Fogo Seamounts, eastern Canada

G. Pe-Piper, A. de Jonge, D.J.W. Piper, L.F. Jansa

2006

Available from
Geological Survey of Canada, Atlantic
1 Challenger Drive
Dartmouth, Nova Scotia B2Y 4A2

Pe-Piper, G., de Jonge, A., Piper, D.J.W., Jansa, L.F.
2006: Morphology, petrography, age and origin of the Fogo Seamounts, eastern Canada, Geological Survey of Canada, Open File 5182, 76 p.

Open files are products that have not gone through the GSC formal publication process.

Preface

This Open File is a compilation of data on the Cretaceous Fogo Seamounts, that form the eastern limit of the Scotian Basin of eastern Canada. A preliminary interpretation of the data is also provided.

Acknowledgments

This work was a cooperative study between Saint Mary's University and the Geological Survey of Canada. Georgia Pe-Piper's work was supported by an NSERC Discovery Grant. Ashley de Jonge was supported by an NSERC summer student award and this Open file is based on her work report. Hudson cruise 91020 was supported by the Geological Survey of Canada through the Program for Energy R&D (PERD), sub-project 532211. Manuscript reviewed by Ruth Jackson and Chris Jauer.

Authors' addresses

Georgia Pe-Piper and Ashley de Jonge*
Department of Geology, Saint Mary's University, Halifax, Nova Scotia, B3H 3C3, Canada
gpiper@smu.ca
(* present address: Encana Corp., 150 - 9th Ave SW, P.O. Box 2850, Calgary, Alberta, T2P 2S5, Canada)

David J.W. Piper and Lubomir F. Jansa
Geological Survey of Canada (Atlantic), Bedford Institute of Oceanography, P.O. Box 1006, Dartmouth, N.S., B2Y 4A2, Canada
dpiper@nrcan.gc.ca; lujansa@nrcan.gc.ca

Abstract

The Fogo Seamounts are located approximately 500 km offshore from Newfoundland to the southwest of the Grand Banks of Newfoundland. This complex seamount chain is Early Cretaceous in age and is partially buried under later continental slope deposits. The seamounts are developed along the northeastern transform margin of the Jurassic central Atlantic Ocean. The Narwhal F-99 well was drilled in 1986 on the continental slope into one buried seamount. In this study, we have compiled unpublished data on the bathymetry, seismic-reflection character, and distribution of the Fogo Seamounts and interpret new petrographic, geochemical and geochronological data from a dredge sample from seamount G in the central part of the seamount chain and from the Narwhal F-99 well.

Petrographically, the seamount samples consist of vitrophyric basalt, with clinopyroxene at Narwhal and kaersutite in the dredge sample. Chemically, the samples are olivine basalt with a low Mg number and low concentration of transition metals. Trace element and REE abundances are similar to those of other early Cretaceous volcanic rocks on the southeast Canadian margin, except that LILE are more enriched in basalts on the continental shelf. Sm/Nd isotopes suggest mantle derivation, with ϵ_{Nd} ranges from 2.3 to 4.7. Overall, the Narwhal basalts are more tholeiitic whereas the basalts at seamount G are more alkalic, showing OIB characteristics, and their range of compositions is well matched by basalts from Hawaii.

The dredge sample at seamount G gave a $^{40}Ar/^{39}Ar$ age of 130.3 ± 1.3 Ma on kaersutite (top Hauterivian on the Gradstein et al. 2004 time scale). A K/Ar age from the Narwhal F-99 well of 127 ± 6 Ma is inconsistent with biostratigraphic zonation, which shows that sedimentary rocks overlying basalt in the well are at least as old as early Berriasian (ca. 145 Ma). Seismic reflection profiles show that a series of coastal transgressions can be recognised above the basalt, with final submergence probably in the Berriasian.

Distribution of the seamounts, based on bathymetry and in the case of buried seamounts, magnetic and seismic data, shows that there is no clear linear trend, but rather a broad zone within which seamounts have formed. New bathymetric data shows that flat tops to seamounts, resulting from coastal erosion prior to subsidence and platform carbonate deposition, show no systematic pattern. The broad extent of the seamounts on the margin probably results from the influence of a series of upper crustal faults along the transform margin.

CONTENTS

Introduction

The Fogo Seamounts are located approximately 500 km offshore from the island of Newfoundland, to the southwest of the Grand Banks of Newfoundland (Fig. 1a). This seamount chain of mafic volcanic rocks is considered to be of Early Cretaceous age (Pe-Piper et al. 1990) and is partially buried under later continental slope deposits. The seamounts are developed along the northeastern transform margin of the Jurassic central Atlantic Ocean (Keen et al. 1990) and are approximately sychronous with the early oceanic spreading between the Grand Banks and Iberia (Fig. 1b). The Narwhal F-99 well was drilled in 1986 on the continental slope into a buried seamount. To the southeast of the main Fogo Seamount chain, DSDP Hole 384 was drilled into a seamount on the J-Anomaly Ridge (Tucholke, Vogt et al. 1979). The New England (Duncan 1984) and Newfoundland (Sullivan and Keen 1977) seamount chains are of similar age and also lie offshore southeastern Canada (Fig. 1).

Two hypotheses have been proposed for the origin of the linear seamount chains off eastern Canada (Fig. 2). The "plume model" proposes that magma was produced locally by one or more mantle hot spots, and the relative motion of the lithosphere and mantle resulted in a seamount chain. This model has generally been applied to the New England and Newfoundland seamounts and was extended to the Fogo Seamounts by Duncan (1984). The "leaky fault model" proposes that magma was generated by extension and percolated upward along transform faults (cf. Leake, 1990). This model has been suggested for the New England Seamount chain by Pe-Piper and Jansa (1987).

Purpose of this study

The Fogo Seamounts have not been systematically analyzed since a brief discussion by Sullivan and Keen (1977, 1978). The purpose of this study is to document and bring together available data relating to the character and origin of the Fogo Seamounts. Available unpublished data includes: (1) industry seismic-reflection profiles; (2) new single channel seismic-reflection profiles over some of the seamounts; (3) new bathymetric data and some manuscript bathymetric maps; (4) geochemical, petrographic and isotopic data from the Narwhal F-99 well and from dredge sample 91020-058 from seamount G, from which a radiometric age was also determined.

In this study, we analyzed seismic-reflection and bathymetric data to document geographic variability in the size and elevation of the seamounts (particularly those that resemble

guyots, with flat tops). We use this information to make inferences on the relative age and style of extrusion of the seamounts. We examine sea-level change and its relationship to seamount evolution using data from buried seamounts beneath the continental slope. The geochemistry of samples is compared with that of Cretaceous volcanism elsewhere on the southeastern Canadian margin. A synthesis of the volcanic affinity and history of the seamounts is proposed.

Regional setting

The Scotian Shelf lies on the central part of the eastern North American margin, which has been built over the fractured edge of the North American continental plate in response to the Mesozoic opening of the North Atlantic. Several sedimentary basins developed along the margin which are filled with as much as 12 km of Mesozoic-Cenozoic sedimentary rocks (Jansa and Wade, 1975; Wade and MacLean, 1990).

The volcanic Mesozoic igneous rocks off Eastern Canada have been stratigraphically and radiometrically dated and suggest two distinct episodes of volcanic activity that record the major periods of rifting. The first period of volcanism is associated with the late rifting stage and is dated ~ 200 Ma (Dunning and Hodych, 1990). Basalts were extruded onto the Late Triassic-Early Jurassic continental red beds in the Bay of Fundy and similar grabens in New England, New Jersey, and North Carolina (Jansa and Pe-Piper, 1985; Puffer, 1994). Oceanic rifting between Africa and Nova Scotia began in the Middle Jurassic, with a transform margin along the southwestern Grand Banks (Klitgord and Schouten, 1986).

Superimposed over the first period of rifting on the southern Grand Banks is a second rifting period, related to extension between the Grand Banks and the Iberian peninsula, during the latest Jurassic – Early Cretaceous. It resulted in the Avalon Uplift and the complex Avalon Unconformity. This rifting sequence terminated extensive development of shallow water carbonate which were replaced by clastic deposition in the South Whale subbasin and the Carson and Jeanne d'Arc basins.

The basins around the Grand Banks trend northeast-southwest. They formed initially during the Late Triassic and Early Jurassic rifting, but were reactivated by Early Cretaceous strike-slip motion (Sinclair 1995) at the same time as the Orpheus Graben (Fig. 3) (Weir-Murphy 2004; Pe-Piper and Piper, 2004). The Orpheus Graben is a narrow, fault-bounded basin that deepens and widens eastward from Chedabucto Bay. The transform faults that define the margin of the SW Grand Banks appear to merge with the Cobequid-Chedabucto fault zone in the

Orpheus Graben area, where there was active deformation and volcanism in the Early Cretaceous (Jansa and Pe-Piper, 1986; Pe-Piper and Piper, 2004; Weir-Murphy, 2004). The Orpheus Graben is filled by as much as 10 km of Mesozoic-Cenozoic sedimentary rocks. It is separated on one side by a boundary fault that separates the graben from the southern edge of the Scatarie Ridge (Fig. 3). The fault is a southward dipping, deep crustal listric fault, and may mark the boundary between the Avalon and Meguma terranes, with the fault rejuvenated by Triassic rifting (Pe-Piper and Jansa, 1999).

Offshore, the J-Anomaly ridge and Southeast Newfoundland ridge (Fig. 4) are volcanic structures south of the Grand Banks (Sullivan and Keen, 1978). The J-Anomaly ridge is parallel to the magnetic stripes produced by spreading at the central Atlantic Mid-Ocean Ridge. It represents enhanced extrusive activity at the ridge in Aptian time (Tucholke, Vogt et al. 1979). The Southeast Newfoundland Ridge is oblique to the J-Anomaly ridge and extends about 900 km southeast from the Tail of the Banks (Grant and McAlpine, 1990). The origin of this ridge is disputed due to the lack of geophysical data, but it have formed from transpression or localised volcanism along complex transform fault, modified by later sedimentation that was largely controlled by bottom currents.

Cretaceous volcanic rocks are widespread on the southeast Canadian margin, best known in the Orpheus Graben and the southwest Grand Banks. The stratigraphy of the igneous sequences in the wells in the Orpheus Graben (Hercules J-15, Jason C-20 and Argo F-38) has been inferred from study of the cuttings and wire-line logs, and two igneous units are distinguished (Jansa and Pe-Piper, 1985). The lower unit consists of principally holocrystalline basalt or diabase in thick bodies . The upper unit has a much more varied composition that includes pyroclastic or volcaniclastic rocks and siliciclastic sedimentary rocks, intercalated with thin basalt and trachyte. The lower unit occurs within the middle Missisauga Formation and could be intrusive. However, Lyngberg (1984) noted that spores immediately below this interval were darker in colour, but not above, suggesting a flow origin. The upper unit, which is clearly extrusive, occurs at the base of the Cree Member of the Logan Canyon Formation (Weir-Murphy, 2004). Similar basalt (or diabase) is found in the Hesper I-52 well on the southeastern Scotian Shelf. A continuous seismic marker from Hesper to the Orpheus graben volcanics (Weir-Murphy, 2004) suggests that the Hesper rocks are flows, contrary to the original interpretation of Jansa and Pe-Piper (1985). Drillcore samples from diabase dykes on Scatarie Ridge, north of Orpheus graben, are geochemically similar to basalt from Orpheus Graben (Jansa et al. 1993).

On the southwest Grand Banks, Cretaceous volcanic rocks were encountered in the Brant P-87, Mallard M-45, Twillick G-49 and Emerillon C-56 wells (Fig. 4). Cuttings samples from the Brant P-87 well indicate the presence of at least five flows or sills of fine-medium crystalline basalt, at two stratigraphic levels, separated by an interval in which tuffs and other pyroclastic rocks predominate (Jansa and Pe-Piper, 1988; Pe-Piper et al. 1994). Biostratigraphic data and seismic correlation with other wells in the Whale subbasin indicate that the lower basalt unit and the felsic unit were extruded during deposition of the Lower Cretaceous Missisauga Formation, in the Neocomian. The upper basalt unit overlies sedimentary rocks containing late Barremian foraminifera (Gradstein, 1977) and palynomorphs (Davies, 1984). A whole rock age of 135±6 Ma (Table 1) from the lower basalt unit corresponds to Hauterivian or Valanginian on the Gradstein et al. (2004) time scale.

No volcaniclastic sediments have been found associated with the mafic rocks in the Twillick G-49 well. From the changes in crystallinity and the weathering profile at the top, the mafic rocks are inferred to be either a sill or more probably a thick subaerial flow, which the well did not completely penetrate. Weathering and soil-profile development indicate that the unit was emplaced before or at the time of an unconformity, which separates Upper Aptian from Turonian rocks in this well (Amoco Canada Petroleum Company Ltd., 1974). A whole rock K-Ar age of 117±5 Ma (Aptian) was obtained from the diabase.

The igneous rock body in the Emerillon C-56 well is a light-grey holocrystalline porphyritic monzodiorite that intrudes a middle Jurassic clastic sequence (Ascoli, 1981). A K-Ar age of 96.4±3.8 Ma (early Cenomanian) was obtained on biotite from a monzodiorite sample (Table 1).

The Mallard M-45 well bottomed at 3522 m in Jurassic limestone. A major base-Cretaceous unconformity at 3220 m (biostratigraphically dated, MacLean and Wade, 1993) separates the base of the volcanic sequence from the underlying late Jurassic limestone. The volcanic sequence, 951.6 m thick, is lithologically heterogenous and may be divided into four units that appear to be principally extrusive (Pe-Piper et al. 1994). K-Ar dating gave ages of 127±4 and 128±3 Ma for basalt and 133±3 and 134±3 Ma for felsic rocks (Table 1). The overlying mid-Cretaceous unconformity is overlain by the Eider Member, which is of late Albian age at the Heron H-73 well (Williams, in MacLean and Wade 1993).

Geophysical data

Bathymetry

The Fogo seamounts are located in deep water off the continental shelf of the Grand Banks. Bathymetric data compiled by the Atlantic Geoscience Centre for the Grand Banks Basin Atlas show the principal geological structures in the area (Fig. 4). These data are partly from Canadian Hydrographic Service compilations, partly from the ETOPO5 database of Heirtzler et al. (1985), and partly from compilations by Piper and Sparkes (1990) and Piper et al. (1995).

The flat continental shelf of the Grand Banks of Newfoundland terminates abruptly at a steep continental slope incised by canyons. The continental slope leads to a flatter continental rise below about 3000 mbsl. The Southeast Newfoundland and J-Anomaly ridges, formed by volcanic activity, have tops 500-1500 m above the regional seafloor. The Fogo seamounts are visible as discrete bathymetric features north of the J-Anomaly Ridge, but to the north and east are partially buried by continental slope sedimentation. The seamount crests are at a depth of 2000 to 4000 mbsl, with the adjacent ocean floor away from the continental slope at depths of 4500 to 5000 mbsl.

There have been several cruises over the seamount area that conducted 12 kHz bathymetric surveys (Fig. 5). These cruises include: Hudson 91020, 87008, 75009 phase 2, 74021, 73011, and 72021. This data allows more precise definition of the bathymetry of some seamounts, although gaps in data were common near seamounts. Only on cruises since 1990 was a 3.5 kHz sounder data available. Navigation on cruises prior to 1990 was by Loran-C and Transit satellite, probably good to ± 100 m in the 1980's and poorer in the 1970's. Later cruises used Global Positioning System, good to better than 10 m.

Typically, bathymetric profiles across larger seamounts show steep flanks and a relatively flatter top, 2 - 10 km across (Fig. 6). Scoured moats or slope channels are found beside some of the seamounts.

Magnetics

Interpretation of the regional magnetic field is based on the Geological Survey of Canada-Atlantic database of marine magnetic data (S. Dehler, pers. comm. 1999). The magnetic anomalies shown in Figure 7 are reduced to the pole. Note that some data is based on 1960's cruises, prior to Loran-C, when offshore navigation was poor.

Many subcircular positive magnetic anomalies correspond precisely to the extent of seamounts recognised from either bathymetric data (Fig. 8) or seismic reflection profiles (e.g., the Narwhal F-99 well). This suggests that positive anomalies can be used to better define the location of seamounts in areas where seamounts are buried by younger sediment. In some cases, the match of magnetics to bathymetry is poorer: this may be due to poor navigation and gridding artefacts in areas of no magnetic data.

Subcircular magnetic anomalies on the continental shelf cannot be seamounts but may indicate volcanic rocks. A weak positive magnetic anomaly is developed near the Brant P-87 and Mallard M-45 wells.

Seismic Reflection Profiles

The seismic reflection profiles studied include sparse regional industry multi-channel profiles (Fig. 9) and Bedford Institute of Oceanography single channel reflection profiles (Fig. 10). Most seamounts on the continental slope are crossed by a seismic-reflection profile but several seamounts in the deeper water in the southwest appear to have no crossing profiles. In order to facilitate discussion, individual seamounts are identified by letters (e.g., B, JJ). These identifiers have been assigned randomly and have no other significance.

The industry multi-channel profiles mostly penetrate to crystalline basement on the Grand Banks and adjacent slope and to oceanic volcanic basement farther seaward. Volcanic basement shows considerable relief (Fig. 11), represented in map form in Figure 12. Single-channel profiles penetrated less deeply and were mainly of value to understanding sediment deposits on the crests of seamounts.

The seamounts, both emergent and buried, generally show steep sides and a flat top (Figs. 11, 13, 14, 15). Commonly it is difficult to distinguish precisely between volcanic basement and reflective sediment on seamount crests, in part because of side echoes (e.g., seamount F, Fig. 11). High-resolution airgun profiles from the crests of some seamounts show quite variable sediment cover on the flat tops (Fig. 16). For example, Seamount G has quite irregular volcanic basement. A build-up on the flank of the seamount with incoherent reflections may be a reef deposit (analogous to DSDP Site 384) with stratified back-reef limestones behind it. This inferred reef may have protected the seamount from further erosion. Overlying stratified sedimentary rocks with high-amplitude reflections might also be of neritic origin. However, overlying more transparent sections with diverging reflections are probably pelagic drift

sedimentary rocks, by analogy with DSDP Site 384. Seamount U has a very similar reef-like build up, capped by a very thin pelagic drift sequence. Seamount FF, in contrast, appears to have relatively flat volcanic basement overlain by 100 ms of fairly transparent pelagic drift sediment. It is possible that this seamount never reached the ocean surface. Industry seismic shows that seamount N (Fig. 15) has 700 ms of overlying sediment, probably mostly pelagic. In comparison, north of DSDP Site 384, pelagic sediment is about 600 ms thick, although at the site itself it is much thinner (Tucholke, Vogt et al. 1979). Buried seamount E (Fig. 13) has about 200 ms of overlying sediment that appears relatively incoherent and may be neritic, unconformably overlain by stratified Quaternary continental rise sediments.

Distribution of the seamounts based on all geophysical data

Using seismics, magnetics and bathymetry, the distribution of both surface and buried seamounts has been mapped and a letter identifier assigned to each seamount (Fig. 17, Table 2). Each of these data sets has its limitations. Ships tracks in the region are sparse and those prior to about 1980 have questionable navigation. As a result, seamounts shown on published bathymetric maps may have errors in positioning. For example, the feature marked H does not exist as a bathymetric feature, even though it is shown on published maps. A further complication is that the widely available map of Tucholke et al. (1986) has erroneous depth contours. In some cases, the presence of a seamount is inferred from a seismic line that only crosses the flanks, so that the true elevation of the seamount is unknown. Figure 13 illustrates a flank section of seamount B; seamount S is intepreted principally from such a flank section, although it also has a magnetic signature. In other cases, the nature of the basement is uncertain: feature II is a buried basement high, but does not appear to be magnetic and is thus probably not a seamount. In most cases, there is insufficient seismic or bathymetric data to define the shape of the seamounts. Magnetic data is gridded from ships tracks and thus has some of the same navigational limitations as the bathymetry. In areas of sparse data coverage, contouring artefacts may be created by the gridding. The prominent magnetic high to the south of the Tail of the Banks (north of JJ and N) has almost no data coverage; the apparent position of seamount U, defined by bathymetry and seismic, in a magnetic low suggests that there are problems with the magnetic data in this area.

The Narwhal F-99 well

The Narwhal F-99 well (Figs. 4, 18a) was drilled in 1573 m water depth on the continental slope in the South Whale Basin into a volcanic basement high, namely a flat-topped seamount or guyot (seamount A in Fig. 17). The well penetrated a thick Cenozoic and Cretaceous section and bottomed in basalt, with the top of the basalt at 4478 mbsl. The volcanic basement is overlain by shallow-water carbonate platform sediments that are abruptly overlain by hemipelagic shales. The gamma log suggests a condensation horizon is developed at the base of the shales, suggesting rapid flooding of the platform.

The lowest definite palynological zonal assignment is early Berriasian at a depth[1] of 4475 m (Bujak Davies Group, 1987), with relatively complete zonation of the Cretaceous above this depth (Fig. 18b). Below this, no zonal assignment is possible and there is evidence of reworking of Late Jurassic species. Foraminifera from 4375-4585 include common Late Jurassic species that were interpreted as reworked by Ascoli (1989). He identified Berriasian foraminifera below 3570 m. Because only cuttings samples were available, except for one conventional core in the Valanginian, only “tops” of stratigraphic markers can be used. Microfauna from the Albian to Campanian are interpreted as outer neritic; Aptian to Hauterivian as middle to outer neritic; and older strata as inner to outer neritic. Tertiary foraminifera indicate a lower bathyal environment (Thomas 1993).

A K/Ar whole rock date of 127±6 Ma (Table 1) was obtained from basaltic basement at the Narwhal well, corresponding to Barremian in the timescale of Gradstein et al. (2004). This radiometric ages appears too young compared with the biostratigraphy (overlying early Berriasian rocks are 145.5 ± 4.0 Ma on the Gradstein et al. (2004) timescale), probably because of argon loss.

Well to seismic correlation is summarized by MacLean and Wade (1993). They identified seismic markers, on the basis of biostratigraphy and regional correlations with the Grand Banks shelf, as the O marker, the Petrel marker, the base Tertiary unconformity and the Mid-Oligocene unconformity (Figs. 17, 19, 20, 21). The O-marker of MacLean and Wade (1993) may be a different horizon from the O-marker in the type section on the Scotian Shelf, where it is of Hauterivian to Barremian age. In the Narwhal well, the O-marker picked by MacLean and Wade (1993) is of Berriasian age, based on both foraminifera and palynomorphs (Fig. 18).

[1] depths in metres (m) are below RT; subtract 24 m to convert to mbsl.

Both the O and Petrel markers are regionally planar horizons represented by highstand limestones. The O-marker and two higher horizons within the Berriasian to Valanginian part of the section show abrupt inflections seaward of the Narwhal well and underlying inclined reflectors are eroded out in a toplap relationship (Figs. 20, 21). The inflection points appear to represent paleoshoreline of lowstand progradational deposits, with onlap of basinal sedimentary rocks in deeper water. They thus provide control on the subsidence of the Narwhal seamount through the early Cretaceous (Fig. 22). The Petrel marker also shows an inflection point in one seismic section, but lacks evidence of toplap. Benthic foraminifera suggest an outer neritic environment for this part of the section. The base-Tertiary marker also appears to be a planar, but the mid-Oligocene unconformity is quite different in character and is strongly down-cutting, suggesting that it developed in a submarine environment by canyon widening on the continental slope.

Geochronology of other seamounts in the Fogo seamount chain

Other than the Narwhal well, geochronology is available only from a dredge sample (91020-058) from the flanks of seamount G, where kaersutite from a basalt clast gave an $^{40}Ar/^{39}Ar$ age of 130.3 ± 1.3 Ma (Table 1), equivalent to Hauterivian-Barremian boundary in the Gradstein et al. (2004) timescale.

The voluminous volcanism of the J-Anomaly Ridge has been interpreted as thickened oceanic crust analogous to the Reykjanes Ridge south of Iceland (Tucholke and Ludwig 1982). Tholeiitic basalt from the base of DSDP Site 384 on the J-Anomaly Ridge is of late Barremian to early Aptian age based on magnetostratigraphy. This is overlain by 122 m of bioclastic (reef) limestone of Aptian to late Albian age. A 10 m coring gap separates the top of the reef from a thick section of Maestrichtian chalks. The presence of a trace of Coniacian-Santonian nannofossil ooze at the top of the reef section suggests a condensed upper Cretaceous deep-water section, implying rapid post-Albian subsidence (Tucholke, Vogt et al., 1979).

Petrology of the rocks from the Fogo seamount chain

Dredge 91020-058

A sample of basalt conglomerate with a calcareous matrix (Fig. 23) was obtained from dredge 058 from the flanks of seamount G (Figs. 4, 17). The clasts are of five main lithologic groups based on their colour and texture (Fig. 24). Group A is a light grey basalt with amygdules filled with calcite (Fig. 24A). Group B is light pink to green-pink lithology. It may be the weathered equivalent of group E and it often contains dark-coloured patches (Fig. 24B). Group C is a dark-coloured lithology (Fig 24C) which consists entirely of megacrysts of amphibole. These crystals are commonly found within the other lithologies and particularly in the B group. Group D is a reddish-brown colour (Fig. 24C and D), occurring as small clasts comprising <5% of the rock (Fig. 24B). Group E, making up 75% of the clasts present, consists of light green basaltic clasts (Fig. 24E), some partly altered to a light pink colour.

Thin section study shows that all five groups consist of amygdaloidal vitrophyric basalt, with subhedral to anhedral phenocrysts of K-feldspar and amphibole set in a trachytic groundmass. The trachytic groundmass is composed of moderately to strongly oriented crystals of feldspar and glass (Table 3). All analysed fresh feldspar crystals were chemically sanidine (Table 3). The amphibole crystals are all kaersutite (Table 4). The opaque minerals range in size and shape and are Ti-magnetite (Table 5) that is commonly altered to hematite. Some of the opaque minerals occur in the groundmass while others are hosted poikilitically by feldspar crystals. The alteration minerals include a variety of smectites, dusty opaque minerals and calcite (Table 6).

Narwhal F-99 well

Samples from the Narwhal F-99 well are in the form of cuttings and were taken at different depths ranging from 4510 to 4585 metres. Thin sections were made from the basalt chips that were in the cuttings.

Sample 4510-20

All chips are fine grained basalts containing mostly plagioclase. Minerals present are plagioclase, clinopyroxene, opaque minerals, calcite, and chlorite, together with glass. Amygdules are also present in most of the chips, usually showing concentric zoning with calcite in the middle followed by chlorite and quartz in the rim. The plagioclase crystals seem to be

fresh, in some chips showing moderate to strong trachytic texture, and compositionally range from bytownite to andesine (Table 7). The plagioclase crystals are skeletal microphenocrysts set in a groundmass of calcite, glass and clinopyroxene. The analysed clinopyroxene crystals are titaniferous augite (Table 8, Fig. 25). Opaque minerals are very abundant in all chips and often are larger than all other minerals.

Sample 4525

All basaltic chips from this depth are fine grained basalts containing skeletal plagioclase. Minerals present are plagioclase, clinopyroxene, opaque minerals, rutile, and calcite, together with glass. The plagioclase in most samples shows a weak to moderate trachytic texture. The groundmass surrounding the plagioclase consists of devitrified glass, calcite and clinopyroxene. Clinopyroxene and plagioclase phenocrysts occur in some chips. These clinopyroxene phenocrysts are subhedral to euhedral. Amygdules occur in almost all the chips and they usually are filled with calcite rimmed with chlorite rimmed with quartz. Opaque minerals are also present in all chips and are evenly distributed. Rutile is a common mineral in some of the chips and usually it is associated with the opaque minerals.

Sample 4530-40

The mineralogy of these fine grained chips is very similar to the most of the Narwhal samples, but they have a higher groundmass content, in some exceeding 80%. Minerals present are plagioclase, clinopyroxene, opaque minerals, rutile, and calcite, together with glass. Phenocrysts and microphenocrysts of plagioclase occur in almost all the chips. The microphenocrysts show a trachytic texture and are skeletal. Phenocrysts of clinopyroxene occur in one or two of the chips and in the groundmass of most chips. Amygdules filled with calcite are abundant and some show the same concentric zoning as in other samples. Calcite is also abundant in the groundmass.

Sample 4570

Minerals present are plagioclase, clinopyroxene, opaque minerals, rutile, and calcite, together with glass. Subhedral clinopyroxene phenocrysts occur in a fine grained groundmass made up of calcite, glass, and skeletal crystals of plagioclase. Amygdules are also common and are filled with calcite and/or a dusty microcrystalline material. Opaque minerals are abundant

and they are evenly dispersed throughout the groundmass. Rutile is a common associate with the opaque minerals. Calcite is a major constituent of the chips, occurring in amygdules and as an alteration product of plagioclase and clinopyroxene. The plagioclase microphenocrysts show a trachytic to subtrachytic texture.

Sample 4580-85

Almost all chips are fine grained basalts containing skeletal microphenocrysts of plagioclase. Minerals present are plagioclase, clinopyroxene, opaque minerals, rutile, and calcite, together with glass. Large phenocrysts of clinopyroxene are present in some of the chips. These clinopyroxene phenocrysts are subhedral to euhedral. The plagioclase in all the chips shows a trachytic to subtrachytic texture. Calcite is a common constituent of the chips and is a main component in the groundmass of most of the chips. Amygdules are also present and are filled with calcite or chlorite. Opaque minerals are very common and abundant in all chips. Rutile is a minor constituent except in one chip where it is abundant. Phenocrysts of plagioclase are also present.

Summary of petrography

In all basalts studied in the Narwhal F-99 well, plagioclase is abundant as phenocrysts, microphenocrysts and in the groundmass, with phenocrysts and microphenocrysts showing trachytic to subtrachytic texture. The groundmass is composed of calcite, plagioclase, clinopyroxene and glass. The glass has been partly altered to chlorite, dusty opaque minerals and quartz and thus is commonly green or dusty in colour. Magnetite is common and has partly altered to hematite. Rutile is an accessory mineral. Amygdules, generally with a concentric zoning of calcite, chlorite and quartz, are common.

Geochemistry of the rocks from the Fogo Seamount chain

Methods

Methods used in this study are similar to those described by Jansa and Pe-Piper (1985). For Narwhal, igneous rocks were separated from cuttings samples by a combination of heavy liquid (tetrabromoethane) flotation and hand picking. Major element analyses of pulverized samples from dredge 058 were by fusion and X-ray fluorescence, whereas for Narwhal samples

electron microprobe analysis was used, following the method developed by MacKay (1981). Trace element analyses of samples with sufficient powder have been made by X-ray fluorescence. Rare earth and other trace element analyses have been made by instrumental neutron activation analysis. Further details of methods and precision are given by Jansa and Pe-Piper (1985).

Whole rock analyses have been made on a total of three samples from dredge 058 and fourteen from the Narwhal F-99 well (Table 9). Many samples derived from well cuttings are too small for XRF trace element analyses (requiring >10 g), so that trace element analysis restricted to those elements that can be determined by instrumental neutron activation analysis. Where XRF analyses have been made, the sample size was usually insufficient for INAA. As a result, various geochemical plots use analyses involving both XRF and INAA elements or even average of all analyses available (e.g. Narwhal well). Analyses of separates from closely spaced interval in the well, however, demostrate that the sample size is sufficiently large to be representative.

Analyses of radiogenic isotopes were made through three laboratories, detailed in Table 10. Methods have been previously published, as noted in Table 10.

Major element chemistry and rock nomenclature

All of the analysed rocks from dredge 058 contain between 44% and 47% SiO_2 on a H_2O- and CO_2-free basis. The reliable interstitial glass analyses from the same rocks average about 50% SiO_2 (Table 3). All of the analysed rocks from the Narwhal well contain between 50% and 52% SiO_2, again on a H_2O- and CO_2-free basis. In the IUGS nomenclature (LeBas et al. 1986) the rocks from the dredge 058 fall in the tephrite field (Fig. 26), whereas the Narwhal rocks fall in the basalt fields, with some samples on the border with basaltic andesite (Fig. 26).

The low Mg number of samples from dredge 058 and the Narwhal F-99 well and the low concentrations of the transition metals (Table 9) indicate that none of these rocks represents primary magmas; all have probably experienced a significant amount of fractional crystallization. Although in some rocks the Mg number might have been reduced by alteration (probably the case for the whole rock analyses of the dredge 058 samples), the samples from Narwhal well appear fresh, as do the reliable interstitial glass analyses from the dredge 058 samples.

The dredge 058 samples in their major elements seem to be similar to lavas from the New England Seamounts and in a number of elements such as Al_2O_3, TiO_2, MgO and CaO to

basalt/diabase from the Hesper well (Scotian Shelf) (Fig. 27). The Narwhal samples in their major elements are very similar to the lavas from wells on the Grand Banks, such as Mallard, Twillick, Emerillon and Brant (Fig. 27).

Trace elements

Dredge 058 samples are remarkably similar to the New England Seamounts and Dipper Seamount (in the Newfoundland Seamount chain) in both REE variation (Fig. 28) and the relative abundance of incompatible elements (Fig. 29). Narwhal basalts are distinctly lower in LREE (Fig. 28) and LILE (Fig. 29) compared to Dredge 058 and in this regard closely resemble Brant basalt. Some basalts from Mallard show very similar incompatible element distribution to the Dredge 058, except that Sr is less fractionated.

Radiogenic isotopes

Results of Sm/Nd isotope analyses from Narwhal and dredge 91020-058 (seamount G) are given in Table 10, together with comparative data from other Cretaceous volcanic rocks. Results of Sr and Pb isotopic analysis are given in Table 11. For both Narwhal and seamount G, ϵ_{Nd} ranges from 2.3 to 4.7 with a depleted mantle model age of 0.5 to 0.75 Ga. Both the Newfoundland and New England Seamounts show similar isotopic composition, suggesting that all three have a rather similar mantle source, with the lower ϵ_{Nd} values suggesting some OIB component. Basalt from the Brant well has an even stronger depleted mantle signature, with ϵ_{Nd} of 5.4 and model age of 0.43 Ga. In contrast, correlative volcanic rocks of the Orpheus graben have ϵ_{Nd} of ~1 and a model age of 0.8 Ga, probably as a result of some crustal contamination.

Discussion

Evolution of the seamounts in terms of sea level and subsidence

Some seamounts have flat tops (Fig. 32), whereas others appear to have steep crests. Based on studies of guyots in the Pacific Ocean (Haggerty et al. 1995), flat tops are interpreted to have developed from coastal erosion and carbonate platform growth on seamounts that were initially subaerial, whereas steep crests characterise those that were entirely submarine. Seamounts will subside as a result of the thermally-driven subsidence of oceanic crust on which they were built, with the rate of subsidence dependent on the difference in age between the host

ocean crust and the seamount. Carbonate platform growth may keep pace with subsidence for varying lengths of time and after final submergence, a drape of pelagic sediment will accumulate. Thus detailed interpretation of the significance of a bathymetric flat top requires information from seismic-reflection data (Table 2).

The Narwhal F-99 well and DSDP Site 384 provide insight into the development of flat tops on other seamounts. The top of volcanic basement at Narwhal is relatively flat, in contrast to the steep flanks (Figs. 12, 20). By analogy with Pacific Ocean guyots, this is presumably a result of coastal erosion of the young volcanic edifice and the construction of a carbonate platform, with characteristic (Fig. 18) inner neritic foraminifera. Seismic reflection profiles suggest that coastal or platform erosion conditions prevailed during lowstands certainly to the late Berriasian and perhaps as high as to just below the Petrel marker (Turonian), which drapes a prominent progradational inflection (Fig. 21). There was progressive progradation of the shelf break (shown by arrows in Fig. 21) from the Berriasian to the Turonian. Most upper Cretaceous foraminiferan assemblages, however, are outer neritic and by Eocene, water depths were bathyal. At DSDP Site 384, volcanic basement is again relatively flat. It is overlain by 122 m of Aptian-Albian shallow-water reef limestone followed by a condensed Coniacian-Santonian deep-water section, implying rapid post-Albian subsidence.

It therefore seems probable that other flat-topped seamounts in the Fogo Seamount chain are a consequence of coastal erosion of an emergent volcano, followed by some platform carbonate sedimentation. At Narwhal, neritic sedimentary rocks are 800 m thick, as a result of progradation from the Grand Banks. Farther offshore at Site 384, neritic limestones are 122 m thick. Neritic sedimentary rocks are interpreted to be 0.4 s thick (< 800 m based on velocities at DSDP 384) at seamount G (Fig. 16).

Narwhal F-99 is overlain by early Berriasian or older (possibly Late Jurassic) sedimentary rocks; the dredge sample at Seamount G is of Hauterivian age; and the seamounts of the J-Anomaly Ridge are Barremian to Aptian, based on DSDP Site 384. If seamount subsidence were solely a result of thermal contraction of oceanic lithosphere, then the deepest flat tops to volcanic basement might be expected in the northwest, where the oldest dated seamount is found, although since this is also the area of oldest oceanic crust, the subsidence rate would be less than for seamounts built over younger crust. The sparse available data on the depths to the flat tops of volcanic edifices do not show any systematic pattern (Fig. 32). This suggests an apparently random distribution of volcanism.

Geochemical character of the Fogo Seamounts

Between-sample variation in Sm/Nd isotopes is greater than the differences between Narwhal and dredge 058 at seamount G. Nevertheless, whole-rock geochemical analyses show significant differences between dredge 058 and Narwhal. Dredge 058 is similar to New England and Newfoundland Seamounts geochemically, with rather higher abundances of both LILE and HFSE such as Nb, Zr and Hf compared with Narwhal. Mafic rocks from the Mallard well show the same trends. Narwhal more closely resembles mafic rocks from Brant (with higher ϵ_{Nd}) in having rather lower abundances of both LILE and HFSE, implying tholeiitic character and a more depleted mantle source. Nb and Ta are enriched at Narwhal and Brant compared with the LILE and LREE (Fig. 29), whereas no such relative enrichment occurs in the mafic rocks of the Orpheus Graben wells, which also have higher Ba and Sr and lower ϵ_{Nd} than either the dredge 058 or Narwhal. This suggests greater contamination by crustal material of the Orpheus Graben rocks.

Thus three petrogenetic types of mafic magma are recognised in the area. Rocks at dredge 058 are typical OIB rather alkalic basalts and similar to those in other seamount chains, including Hawaii (Watson, 1993). Rocks at Narwhal and Brant have a greater signature of a depleted mantle source (are more tholeiitic) and resemble tholeiitic basalts from Hawaii. In Orpheus graben, there appears to have been greater crustal contamination, either from the crust in the region or from mantle previously enriched in crustal contaminants.

Tectonic setting of the seamounts

The Fogo Seamounts do not form a well defined linear trend, but form a broad zone of volcanoes across and along the transform margin. This is different from typical seamount chains such as the Newfoundland and New England seamounts. Thus, the Fogo Seamounts probably formed in a more complex manner than typical seamount chains. Although the three available age points on the seamounts might be interpreted to show that the seamounts become younger towards the southeast, the evidence of the flat tops of the seamounts suggests that distribution is more random. The geochemistry shows a contrast between Narwhal and Brant in the north, where more tholeiitic rocks are found, and Mallard and seamount G in the south, where the mafic rocks are similar to ocean-island basalt (OIB) composition.

These geochemical data imply that there was a source of heat that led to some partial melting of asthenospheric mantle or perhaps sub-continental lithospheric mantle to yield the

tholeiites. Ocean-island basalt (OIB) is generally recognised as diagnostic of upwelling deeper asthenosphere (e.g. as reviewed by Greenough et al. 2005). Such upwelling can act as a heat source, although partial melting can also take place by decompression within the rising diapir.

What is unclear is the tectonic origin of these phenomena. The widespread distribution of magmas of differing compositions suggests that a “leaky” transform fault zone played an important role in creating pathways for magma to reach the surface, as suggested by Pe-Piper and Jansa (1987). For the more tholeiitic magmas, it might be that regional crustal thinning due to extension was sufficient to produce magma, but this seems unlikely given the lack of volcanism on the conjugate Galicia margin despite the much greater crustal extension there. Furthermore, in continental areas of much greater crustal extension, extension alone is insufficient to generate a geothermal gradient sufficient to cause partial melting (e.g. Davies and von Blankenburg, 1995). Thus in the case of the Fogo Seamounts, the need to convect heat to cause partial melting and the evidence of OIB geochemistry argue for rising asthenosphere.

Whether mantle plumes are a cause or a consequence of the behaviour of lithospheric plates is a highly controversial scientific issue at present and the data in this report cannot distinguish between the two hypotheses. Several highly speculative geodynamic hypotheses might account for asthenospheric diapirism, including:

a) The classic mantle plume hypothesis, as applied by Duncan (1984), who suggested that the Fogo Seamounts were formed by the passage of the Canary hotspot beneath the Grand Banks.

b) Mantle upwelling could have been initiated by a slab-tear from Tethyan subduction beneath Iberia (cf. de Boorder et al. 1998).

c) Asymmetric mantle upwelling related to ocean opening between Iberia and the Grand Banks, which produced highly asymmetric stretching of continental crust.

d) Rifting of Iberia from the Grand Banks, prior to the separation of Labrador from Europe plus Greenland, resulted in dextral strike-slip in the Jeanne d’Arc basin (Sinclair, 1995) and on the Cobequid-Chedabucto fault system (Pe-Piper and Piper, 2004) beginning at the base of the Cretaceous. The geometry of this system would have produced extensional pull-apart of the area between Narwhal and Sable Island. By analogy with back-arc basins, extension of warm oceanic crust in these areas (less than 30 Myr old) could set up asthenospheric upwelling and tholeiitic magmatism.

Further evaluation of these alternatives is beyond the scope of this Open File report.

Conclusions

1. The Fogo Seamounts do not form a clear linear trend, but instead a broad zone of volcanism across the transform margin. This is different from typical seamount chains e.g. Newfoundland and New England seamounts. The crustal-scale faults of the transform margin facilitated the rise of magma across a broad zone.

2. The depths of flat tops to seamounts (guyots) show no systematic pattern from NW to SE, but may be deeper towards the SW. There are only three age points determined by geochronology and/or biostratigraphy, with the oldest (Narwhal) in the NW and the youngest (DSDP 384) in the SE.

3. Basalts from the Fogo Seamounts show a similar range of compositions to Hawaii basalts. More tholeiitic rocks occur at Narwhal (and Brant); more alkalic basalts at seamount G and Mallard.

4. Both the presence of tholeiitic rocks, implying decompression melting of depleted mantle, and the presence of OIB-type magmas demonstrate that there was upward movement of mantle involved in the magmatism.

References

Amoco Canada Petroleum Company Ltd. 1974: Well history report, Amoco IMP Skelly Twillick G-49. Released to Open File April 1976 by the Department of Energy, Mines and Resources, Ottawa.

Ascoli, P. 1989: Report on the Biostratigraphy (Foraminifera and Ostracoda) and Depositional Environments of the Northcor et al. Narwhal F-99 well (SW Grand Banks), from 3270 to 4585 m (T.D.). Report no. EPGS-PAL.1-89PA, Eastern Petroleum Geology Subdivision.

Bujak-Davies 1987: Palynological Biostratigraphy of the Interval 2320-4570 m, Northcor et al., Narwhal F-99. Geological Survey of Canada Internal Report # 87-0066

Davies, E.H. 1984: Palynological analysis of the Amoco-Imperial-Skelly Brant P-87, South Whale subbasin. Geological Survey of Canada Internal Report EPGS-PAL.7-84EHD, 1p.

Davies, J.H. and von Blanckenburg, F. 1995. Slab breakoff: a model of lithosphere detachment and its test in the magmatism and deformation of collisional orogens. Earth and Planetary Science Letters, v. 129, p. 85-102.

de Boorder, H., Spakman, W., White, S.H., and Wortel, M.J.R., 1998. Late Cenozoic mineralization, orogenic collapse and slab detachment in the European Alpine belt: Earth and Planetary Science Letters, v. 164, p. 569-575.

Duncan, R.A. 1984. Age progressive volcanism in the New England Seamounts and the opening of the central Atlantic Ocean. Journal of Geophysical Research, v. 89, p. 9980-9990.

Dunning, G.R. and Hodych, J.P 1990. U-Pb zircon and baddelyite ages for the Palisades and Gettysburg sills of the northeastern United States: implications for the age of the Triassic/Jurassic boundary. Geology, v. 18, p. 795-798.

Gradstein, F.M. 1977. Biostratigraphy (foraminifera) and depositional environment of Amoco-Imperial-Skelly Brant P-87, Grand Banks. Geological Survey of Canada Internal Report EPGS-PAL.28-77FMG, 5p.

Gradstein, F.M., Ogg, J.G., Smith, A.G., Bleeker, W., and Lourens, L.J. 2004. A new Geologic Time Scale with special reference to the Precambrian and Neogene. Episodes, **27**: 83-100.

Grant, A.C. and McAlpine, K.D. 1990: The Continental Margin Around Newfoundland Chapter 6 in Geology of the Continental Margin of Eastern Canada, M.J. Keen and G.L. Williams (ed); GSC, Geology of Canada, no.2, p. 239-292.

Greenough, J.D., Dostal, J., and Mallory-Greenough, L.M., 2005. Igneous rock associations. 4. Ocean Island Volcanism I, Mineralogy and Petrology. Geoscience Canada, v.32, p.29-35.

Haggerty, J.A., Premoli Silva, I., Rack, F.R. and McNutt, M.K. (eds.), 1995. Proc. ODP, Sci. Results, v. 144, 1059 p.

Hughes Clarke, J.E. 1988. The geological record of the 1929 "Grand Banks" earthquake and its relevance to deep-sea clastic sedimentation. Ph.D. thesis, Dalhousie University, Halifax, N.S., 171 p.

Jansa, L.F., Pe-Piper, G. and Loncarevic, B.D. 1993: Appalachian basement and its intrusion by Cretaceous dykes, offshore southeast Nova Scotia, Canada, Canadian Journal of Earth Sciences, vol. 30, pp. 2495-2509.

Jansa, L.F. and Pe-Piper, G. 1988: Middle Jurassic to Early Cretaceous Igneous Rocks Along Eastern North American Continental Margin. American Association of Petroleum Geologists Bulletin, Vol. 72, No. 3, p. 347-366.

Jansa, L.F. and Pe-Piper, G. 1986: Geology and geochemistry of Middle Jurassic and Early Cretaceous igneous rocks on the eastern North American continental shelf. Geological

Survey of Canada Open File Report No. 1351.

Jansa, L.F. and Pe-Piper, G. 1985: Early Cretaceous volcanism on the northeastern American Margin and implications for plate tectonics, Geological Society of America Bulletin, Vol. 96, p. 83-91.

Jansa, L.F., Pe-Piper, G. and Loncarevic, B.D., 1993. Appalachian basement and its intrusion by Cretaceous dykes, offshore southeast Nova Scotia, Canada. Canadian Journal of Earth Sciences, v. 30, p. 2495-2509.

Jansa, L.F. and Wade, J.F. 1975: Geology of the continental margin off Nova Scotia and Newfoundland; GSC, Paper 74-30, p. 51-105.

Keen, C.E., Loncarevic, B.D., Reid, I., Woodside, J., Haworth, R.T. and Williams, H. 1990: Tectonic and Geophysical overview. Chapter 2 in Geology of the Continental Margin of Eastern Canada, M.J. Keen and G.L. Williams (eds); Geological Survey of Canada, Geology of Canada, no. 2, p. 33-75.

Klitgord, K. D., and Schouten, H. 1986. Plate kinematics of the central Atlantic. The Geology of North America, **M**: 351-378.

Leake, B.E. 1990: Granitic magmas: Their sources, initiation and consequences of emplacement. Journal of the Geological Society of London, vol. 147, p. 579-589.

Louden, K.E., Tucholke, B.E. and Oakey, G.N., 2004. Regional anomalies of sediment thickness, basement depth and isostatic crustal thickness in the North Atlantic Ocean. Earth and Planetary Science Letters, v. 224, p. 193-211.

Lyngberg, E. 1984. The Orpheus graben, offshore Nova Scotia: palynology, organic geochemistry, maturation and time-temperature history. M.Sc. thesis, University of British Columbia, 159 p.

MacKay, R. 1981: Electron microprobe whole rock analysis of basalts. B.Sc. honours thesis, Halifax, Nova Scotia, Dalhousie University.

MacLean, B.C. and Wade, J.A. 1993: Seismic Markers and Stratigraphic Picks in the Scotian Basin Wells. Geological Survey of Canada, Atlantic Geoscience Centre, 276p.

Pe-Piper, G. and Piper, D.J.W. 1999. A test of the broad terrane hypotheses for Jurassic tholeiitic magmas in southeastern Canada. Canadian Journal of Earth Sciences, 36, 1509-1516.

Pe-Piper, G. and Piper, D.J.W., 1998. Geochemical evolution of Devonian-Carboniferous igneous rocks of the Magdalen basin, Eastern Canada: Pb and Nd isotope evidence for mantle and lower crustal sources. Canadian Journal of Earth Sciences, v. 35, p. 201-221.

Pe-Piper, G. and Piper, D.J.W. 2004. The effects of strike-slip motion along the Cobequid-Chedabucto-SW Grand Banks fault system on the Cretaceous - Tertiary evolution of Atlantic Canada. Canadian Journal of Earth Sciences, 41, 799-808.

Pe-Piper, G. and Jansa, L.F., 1987. Geochemistry of late Middle Jurassic- Early Cretaceous igneous rocks on the eastern North American margin. Bulletin of the Geological Society of America, vol. 99, 803-813.

Pe-Piper, G. and Jansa, L.F. 1988: The Origin of Complex Mantling Relationships in Clinopyroxene From the New England Seamounts, Canadian Mineralogist, vol. 26, pp. 109-116.

Pe-Piper, G. and Jansa, L.F., 1999. Pre-Mesozoic basement rocks offshore Nova Scotia, Canada: new constraints on the accretion history of the Meguma terrane. Geological Society of America Bulletin, v. 111, p. 1773-1791.

Pe-Piper, G., Jansa, L.F. and Palacz, Z. 1994: Geochemistry and regional significance of Early Cretaceous bimodal basalt-felsic associations on Grand Banks, eastern Canada, Geological Survey of America Bulletin, vol. 106, p. 1319-1331.

Pe-Piper, G., Jansa, L.F. and Lambert, R. StJ., 1992. Early Mesozoic magmatism on the eastern Canadian margin: petrogenetic and tectonic significance. Geological Society of America Special Paper 268, p. 13-36.

Pe-Piper, G., Piper, D.J.W., Keen, M.J. and McMillan, N.J. 1990. Igneous rocks of the Eastern Canadian continental margin; Chapter 2 in Geology of the continental margin off Eastern Canada, M.J. Keen and G.L. Williams (ed.); Geological Survey of Canada, Geology of Canada, no. 2, p.

Piper, D.J.W., Sparkes, R. and Berry, J., 1995. Bathymetry and echo-character maps of parts of the Scotian Slope and Southwest Grand Banks Slope. Geological Survey of Canada Open File

Piper, D.J.W. and Sparkes, R., 1990. Bathymetry of the continental slope and rise off the southern Grand Banks of Newfoundland. Geological Survey of Canada Open File 2232.

Puffer, J.H. 1994. Initial and secondary Pangean basalts. In: Pangea: Global environments and resources. Edited by: B. Beauchamp, A.F. Embry and D. Glass. Canadian Society of Petroleum Geologists Memoir 17, pp. 85-95.

Robinson, P., Spear, F.S., Schumacher, J.C., Laird, J., Klein, C., Evans, B.W. and Doolan, B.L. 1982: Phase relations of metamorphic amphiboles: Natural occurrences and theory.

Mineralogical Society of America Reviews in Mineralogy, vol. 9B, p. 1-227.

Sinclair, I.K., 1995. Transpressional inversion due to episodic rotation of extensional stresses in Jeanne d'Arc basin, offshore Newfoundland. In: Basin inversion; Buchanan, J.G. and Buchanan, P.G., (eds), Geological Society Special Publication 88, 249-271.

Stout, J.H., 1972. Phase petrology and mineral chemistry of coexisting amphiboles from Telemark, Norway. Journal of Petrology, vol. 13, p. 99-145.

Sullivan, K.D. 1978. The structure and evolution of the Newfoundland basin, offshore eastern Canada. Ph.D. thesis, Dalhousie University, 294 p.

Sullivan, K.D. and Keen,, C.E. 1977. Newfoundland Seamounts: Petrology and Geochemistry. In: Volcanic Regimes in Canada, W.R.A Baragar, L.C. Coleman and J.M. Hall (eds). Geological Association of Canada Special Paper, No. 16, p. 461-476.

Sullivan, K.D. and Keen, C.E. 1978. On the nature of the crust in the vicinity of the Southeast Newfoundland Ridge. Canadian Journal of Earth Sciences, v. 15, p. 1462-1471.

Sun, S.S. and McDonough, W.F. 1990: Chemical and isotopic systematics of oceanic basalts: Implications for mantle composition and processes. In: Saunders, A.D., and Norry, M.J., eds., Magmatism in the ocean basins. Geological Society of London Special Publication No. 42, p. 313-345.

Thomas, F.C. 1993. Northcor et al. Narwhal F-99, southwestern Grand Banks area; Cenozoic foraminiferal biostratigraphy and paleoenvironments. Report BAS-PAL.20-93FCT, internal report, Geological Survey of Canada - Atlantic.

Tucholke, B.E., Vogt, P.R., and shipboard scientific party. 1979. Site 384: The Cretaceous/Tertiary Boundary, Aptian Reefs, and the J-Anomaly Ridge, Deep Sea Drilling Project, v. 43, p. 104-

Tucholke, B.E. and Ludwig, W.J. 1982: Structure and origin of the J-anomaly ridge, western North Atlantic Ocean. Journal of Geophysical Research, v. 87, p.389-9407.

Tucholke, B.E., Raymond, L.A., Vogt, P.R., and Smoot, N.C., 1986. Bathymetry of the North Atlantic Ocean. Plate 2, volume M, The Geology of North America, Geological Society of America.

Wade, J.A. and MacLean, B.C., 1990. Aspects of the geology of the Scotian Basin from recent seismic and well data. Chapter 5, in Geology of the continental margin off eastern Canada, ed. M.J.Keen and G.L.Williams. Geological Survey of Canada, Geology of Canada, no. 2, (also Geological Society of America, The Geology of North America, v. I-

1), p. 190-238.

Wanless, R.K., Stevens, R.D., Lachance, G.R. and Delabir, R.N. 1979: Age determinations and geological studies - K-Ar isotopic ages, report 14. Geological survey of Canada Paper 79-2, 67p.

Wass, S.Y. 1979: Multiple origins of clinopyroxenes in alkali basaltic rocks. Lithos, vol. 12, p. 115-132.

Watson, S., 1993. Rare earth element inversions and percolation models for Hawaii. Journal of Petrology, 32, 501-537.

Weir Murphy, S.L., 2004. Cretaceous rocks of the Orpheus graben, offshore Nova Scotia. M.Sc. thesis, Saint Mary's University.

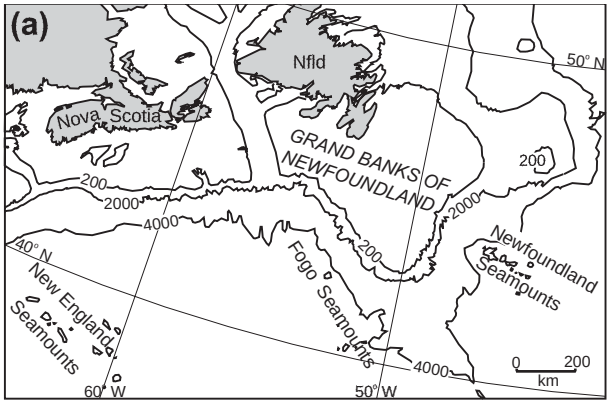

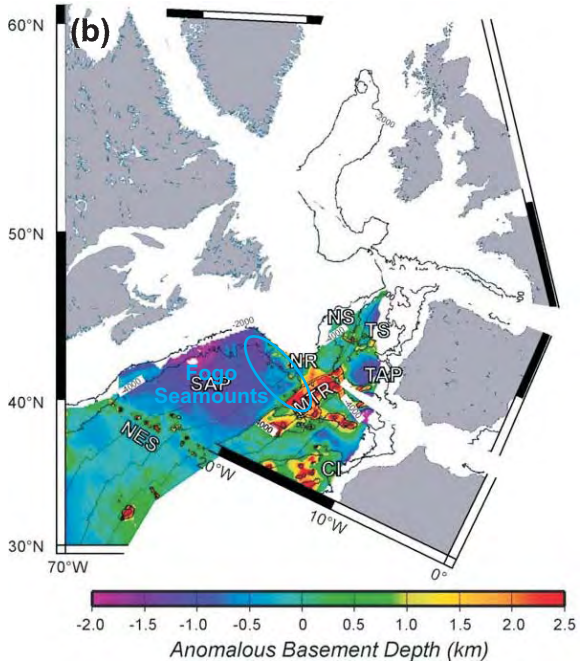

Fig. 1. (a) Map showing location of the Fogo Seamounts and other seamount chains on the southeastern continental margin of Canada. (b) Paleogeographic reconstruction (from Louden et al. 2004) of the North Atlantic Ocean at about the time of formation of the Fogo Seamounts.

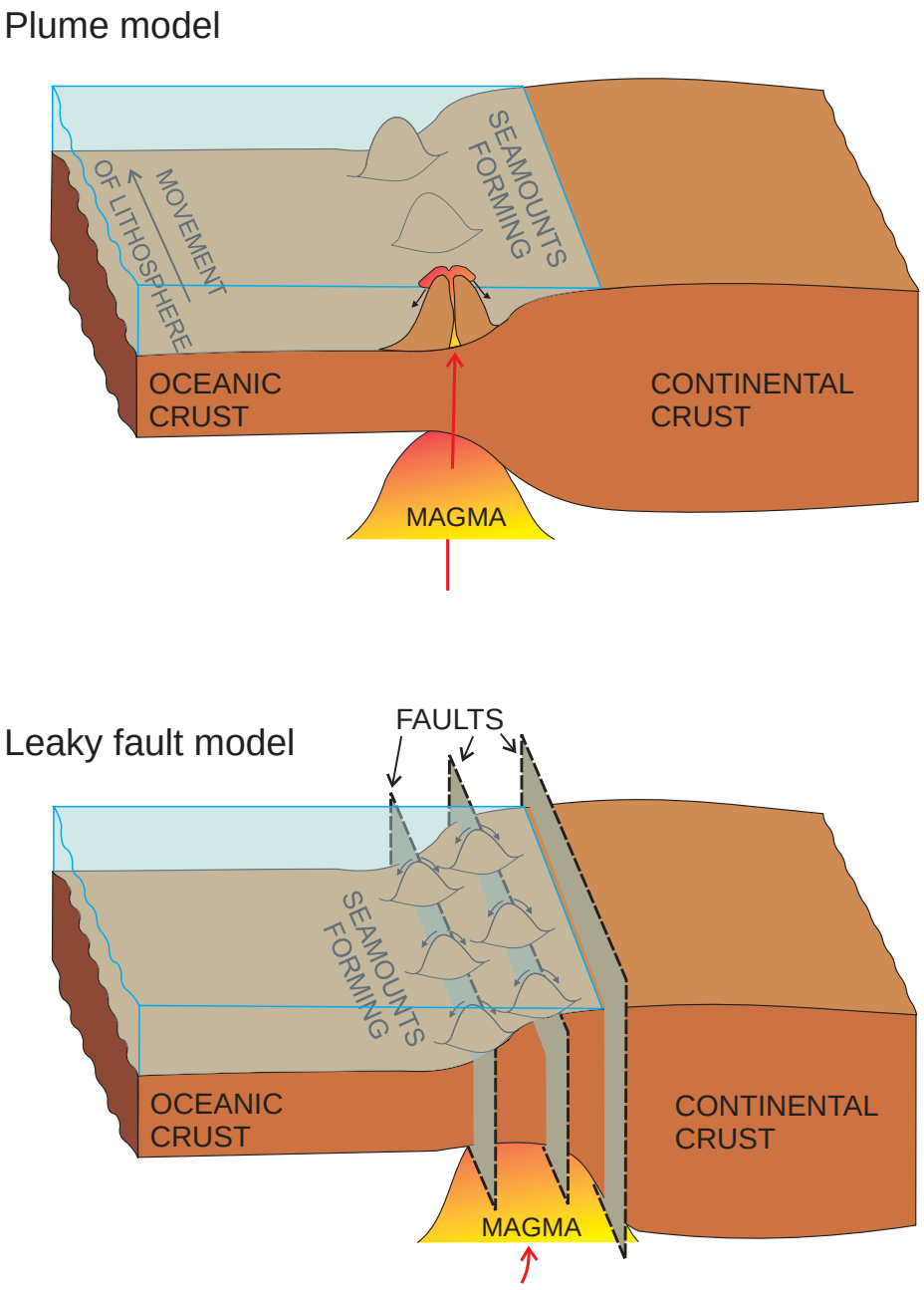

Fig. 2. Cartoon showing the "plume model" and "leaky fault model" for the origin of a linear seamount chain such as the Fogo Seamounts.

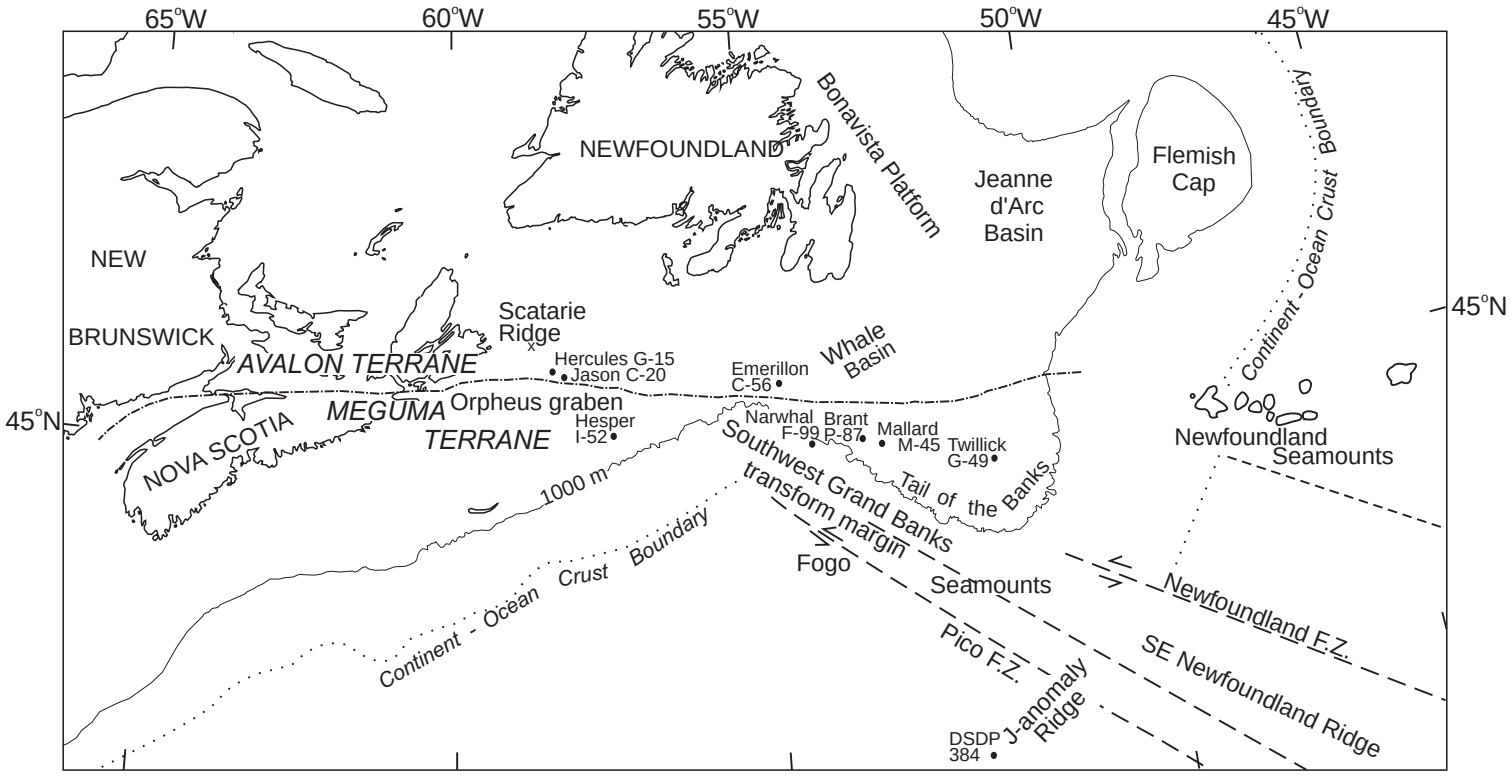

Fig. 3. Regional tectonic setting of the Fogo Seamounts (modified from Jansa et al. 1993 and Pe-Piper and Piper 1999).

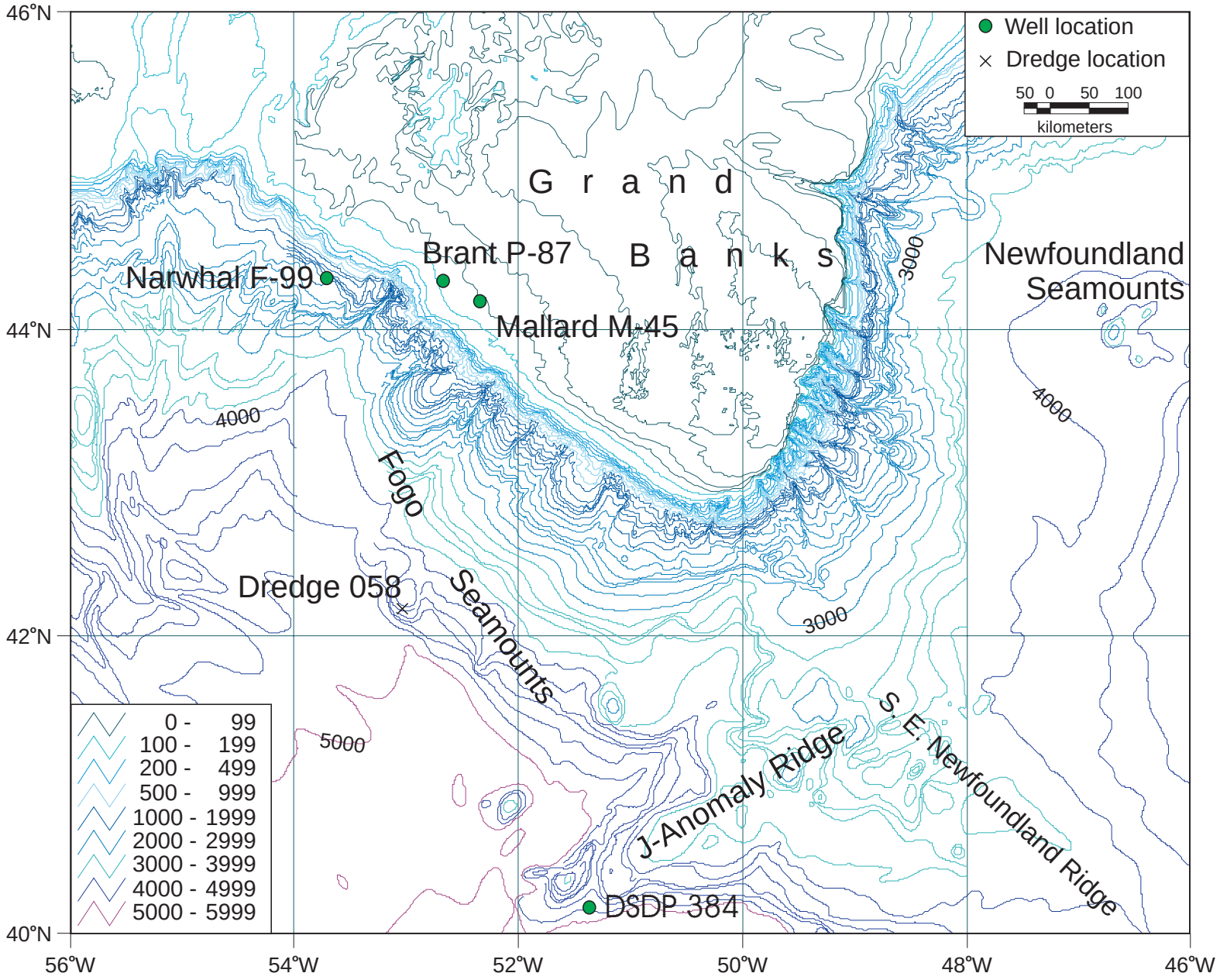

Fig. 4. Bathymetry of Fogo Seamount area, based on the Atlantic Geoscience Centre unpublished Grand Banks Basin Atlas. For further explanation, see text.

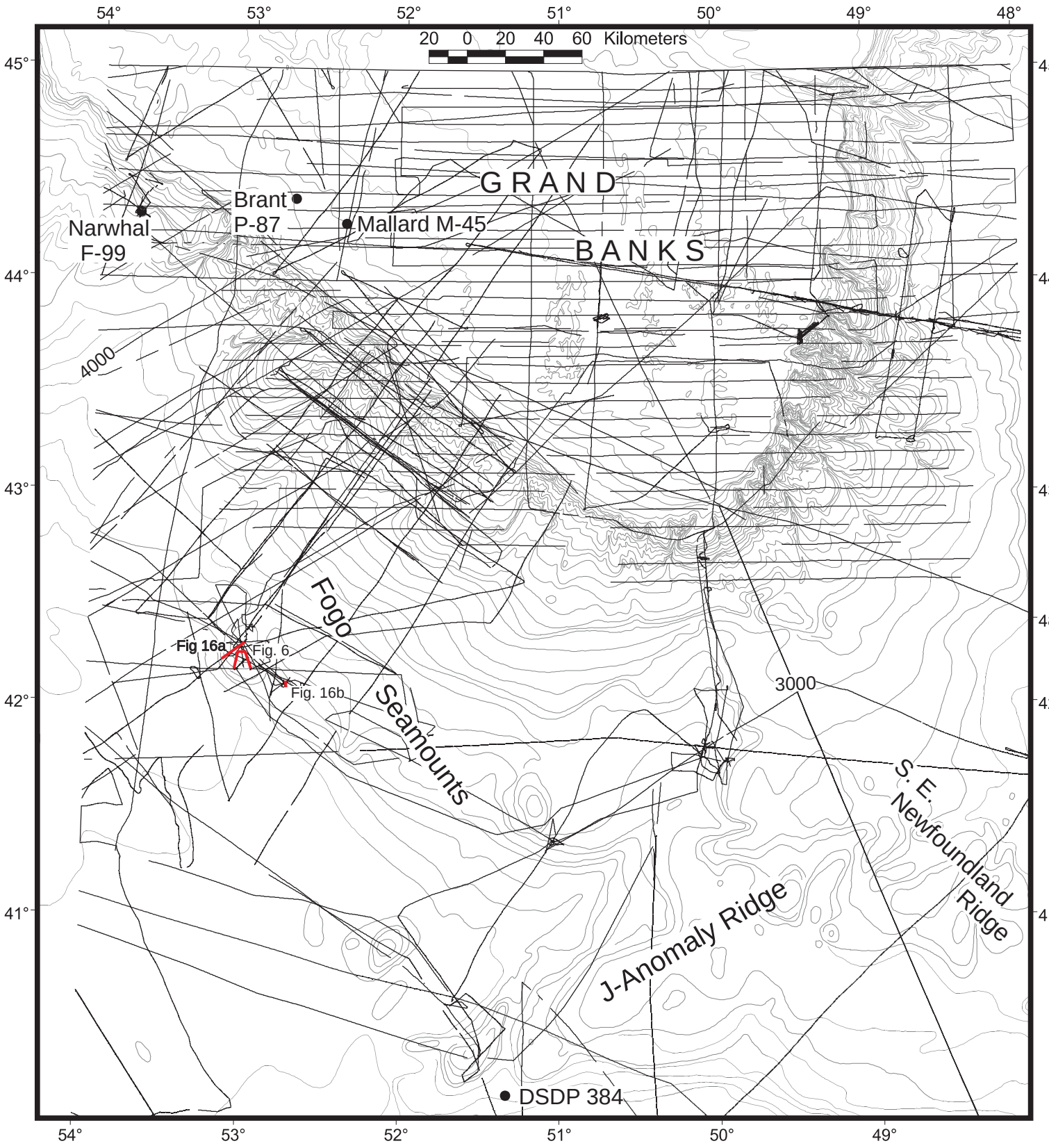

Fig. 5. Map showing distribution of 12 kHz bathymetric profiles at Bedford Institute of Oceanography used to interpret seamount bathymetry.

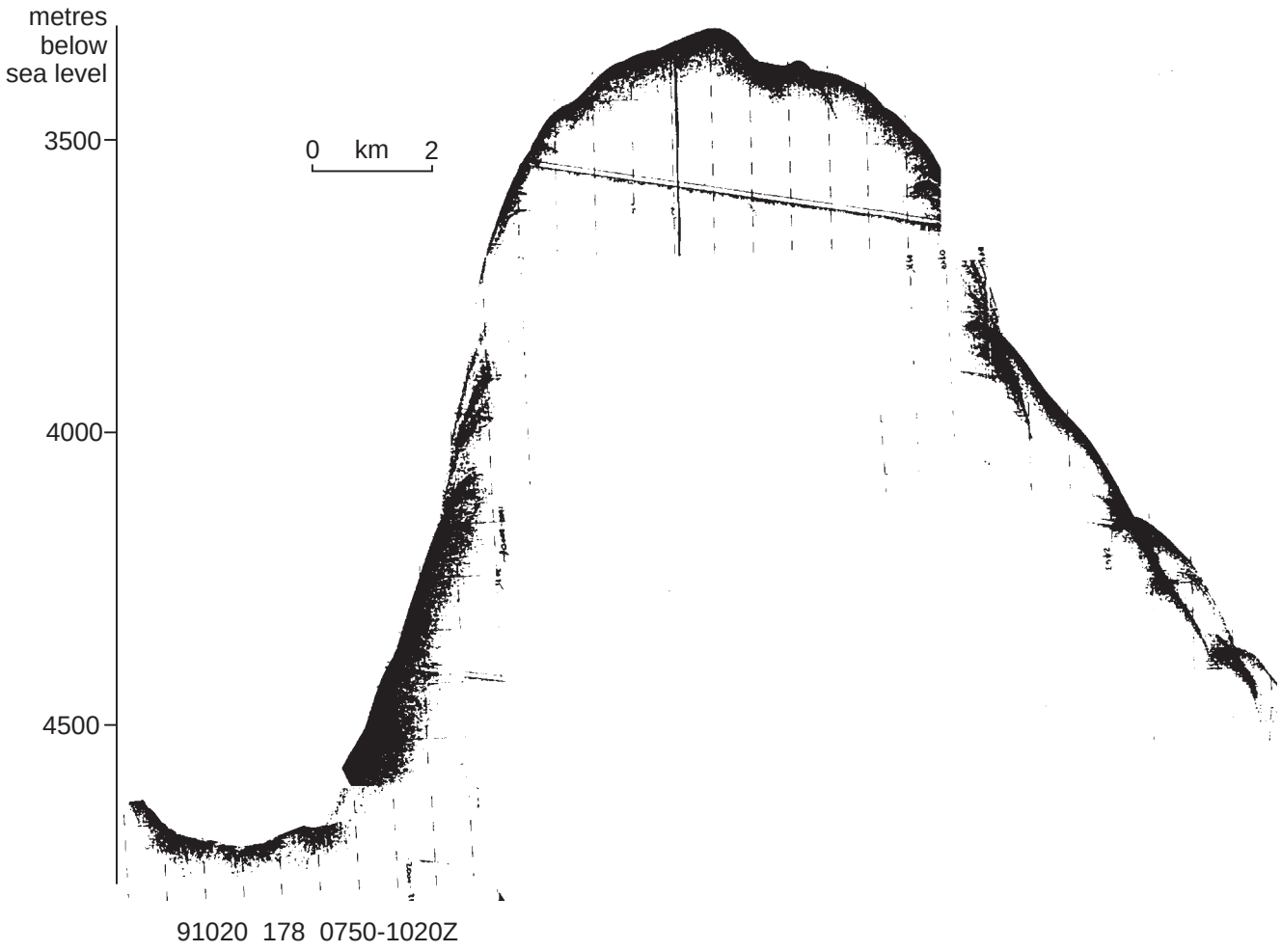

Fig. 6. 12 kHz bathymetric profile across a typical seamount in the Fogo Seamount chain (seamount G) showing flat top to seamount.

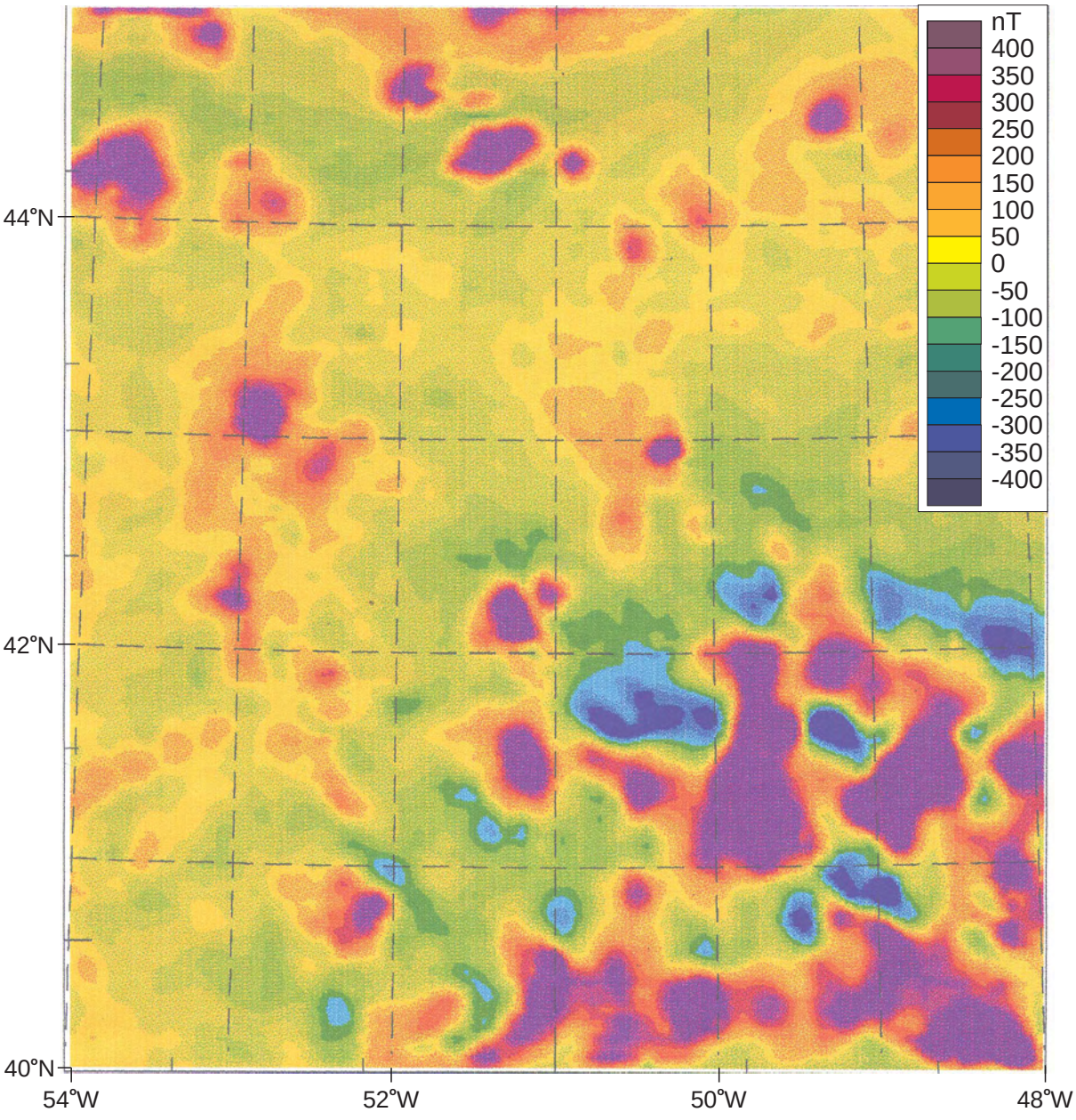

Fig. 7. Magnetic anomaly map (in nannoTesla, reduced to the pole) of the Fogo Seamount area. Map provided by Dr S. Dehler and G. Oakey, Geological Survey of Canada (Atlantic).

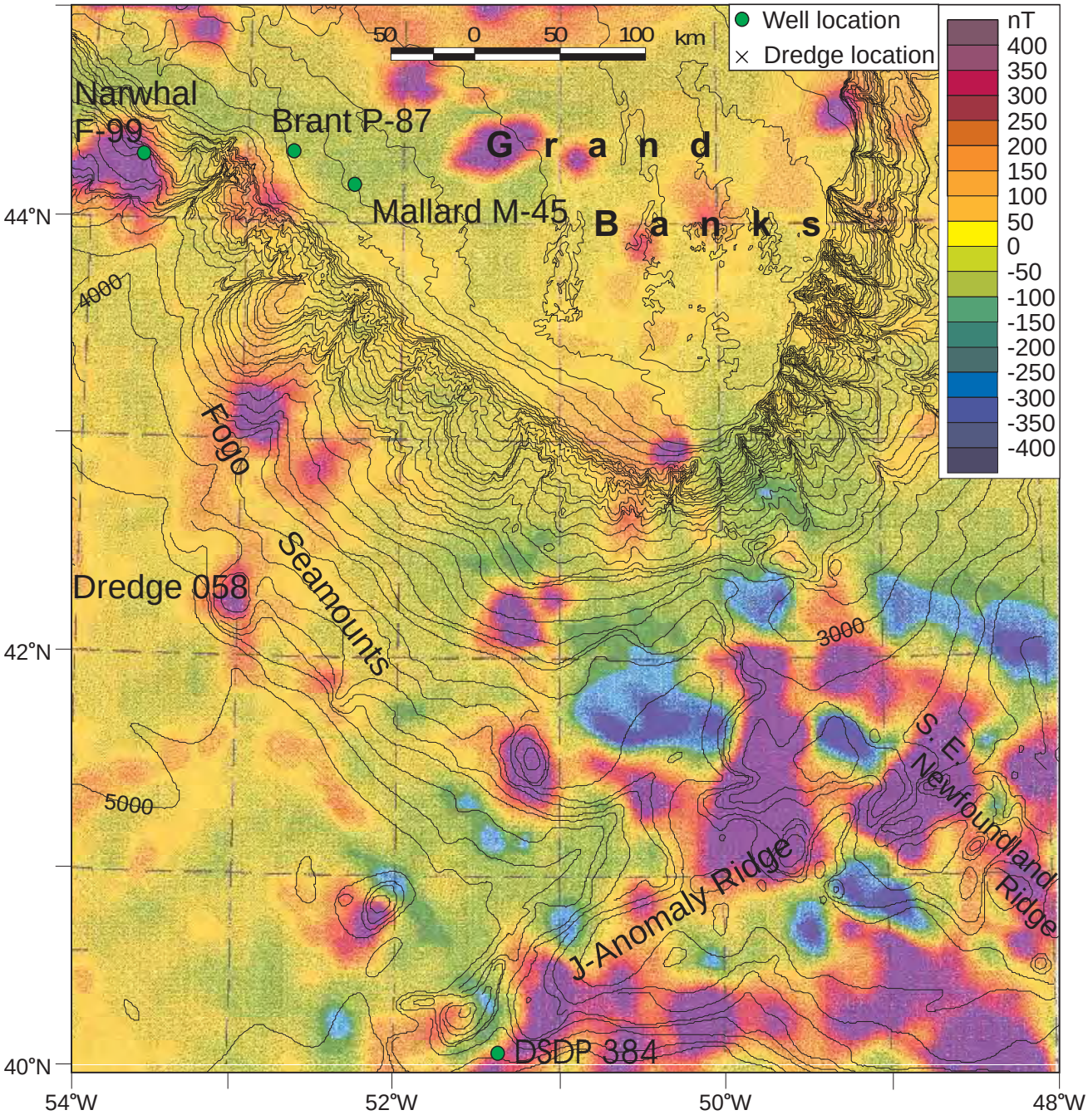

Fig. 8. Magnetic anomaly map superimposed on bathymetry showing relationship of seamounts to positive magnetic anomalies.

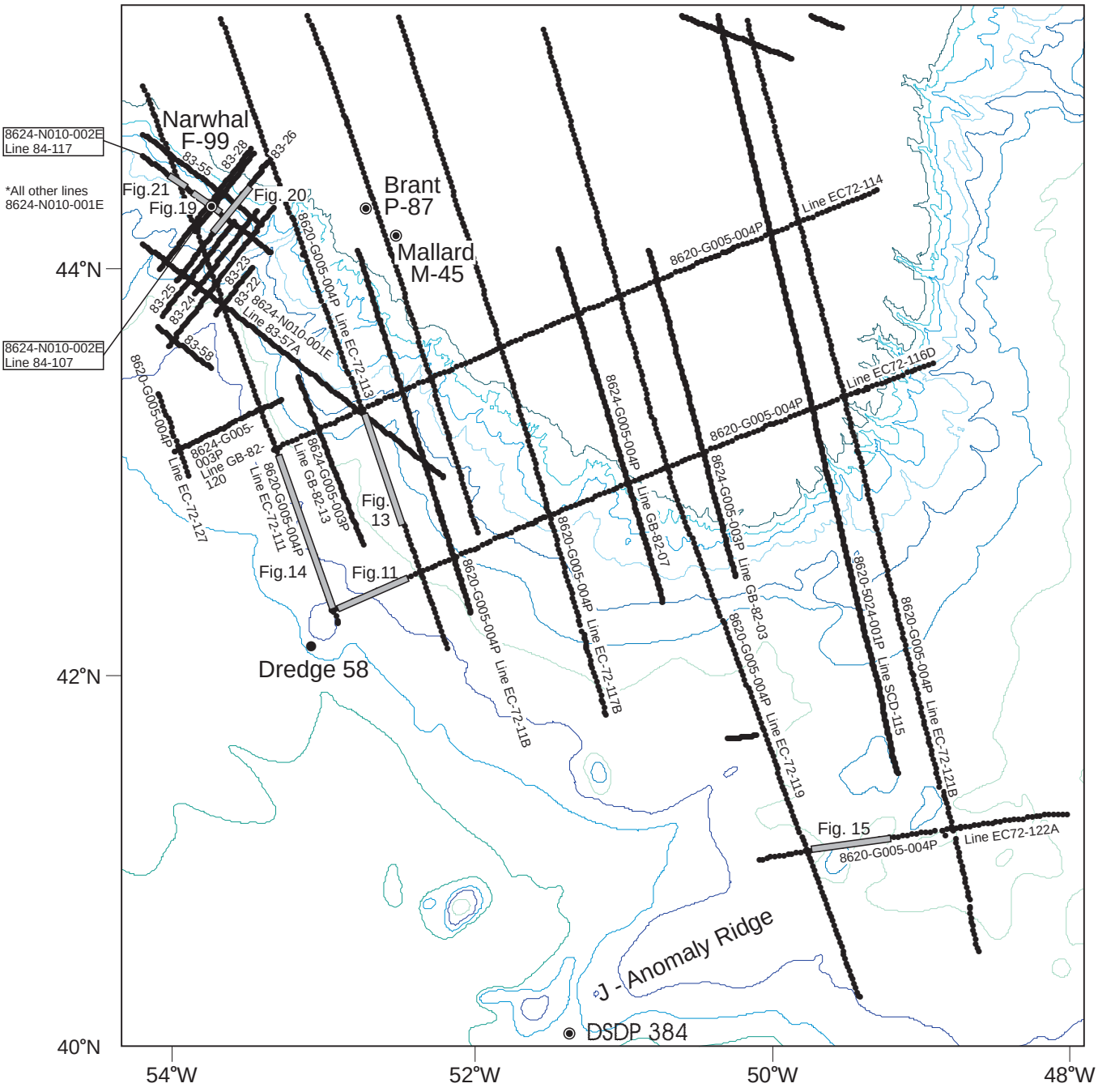

Fig. 9. Industry seismic lines examined for this study. Also shows location of illustrated industry seismic profiles.

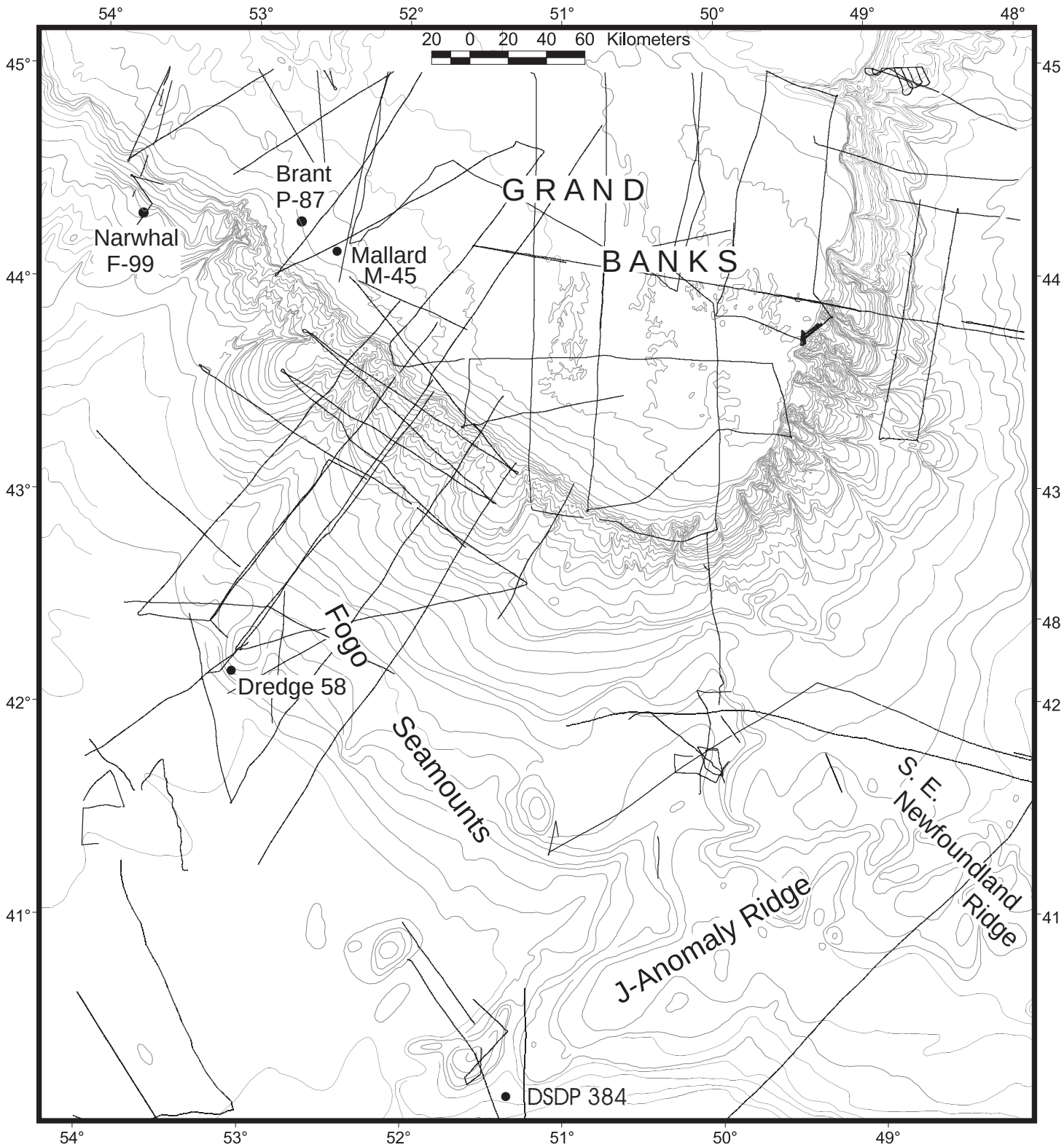

Fig. 10. Single channel seismic lines at Bedford Institute of Oceanography examined for this study. Also shows location of illustrated seismic profiles.

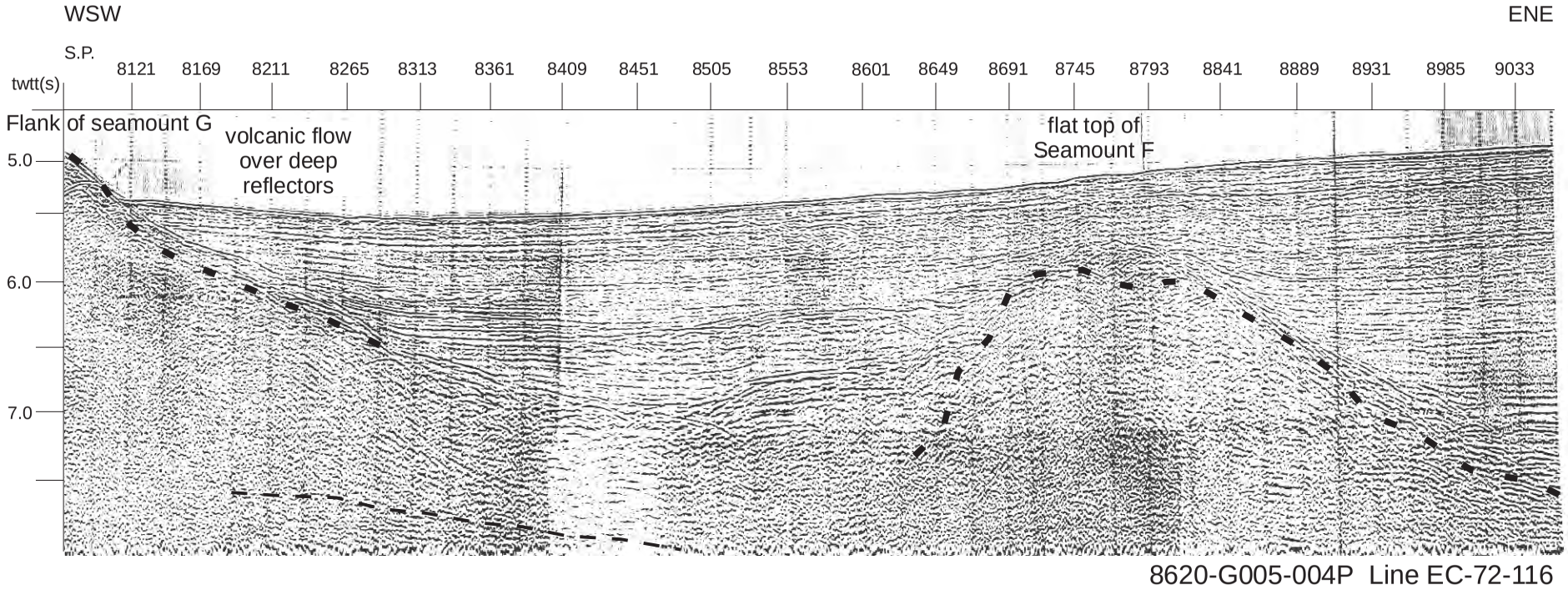

Fig. 11. Seismic reflection profile showing flank of seamount and a lower seamount with a flat top buried beneath the continental rise.

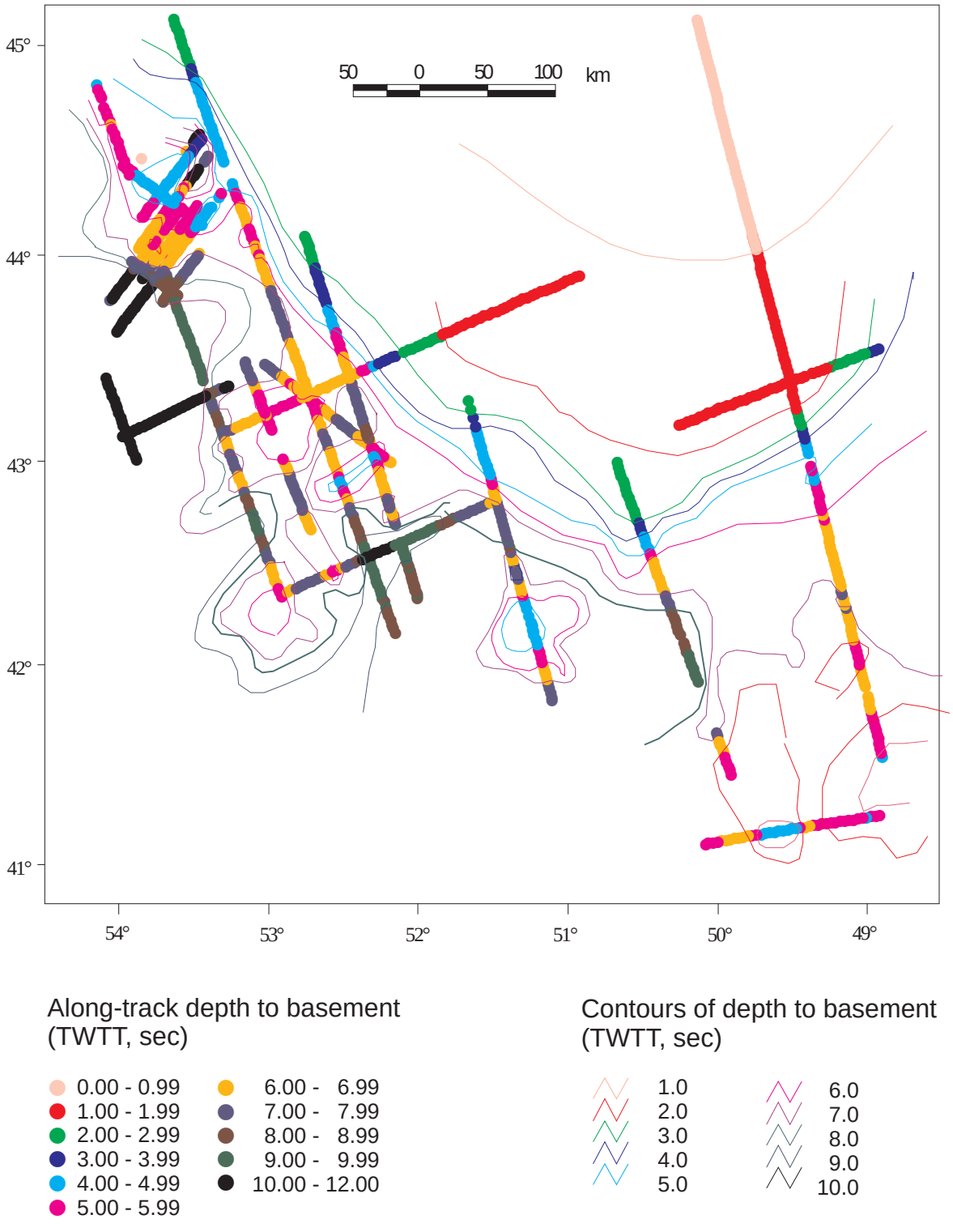

Fig. 12. Depth to basement picked along industry seismic lines (in secs TWTT).

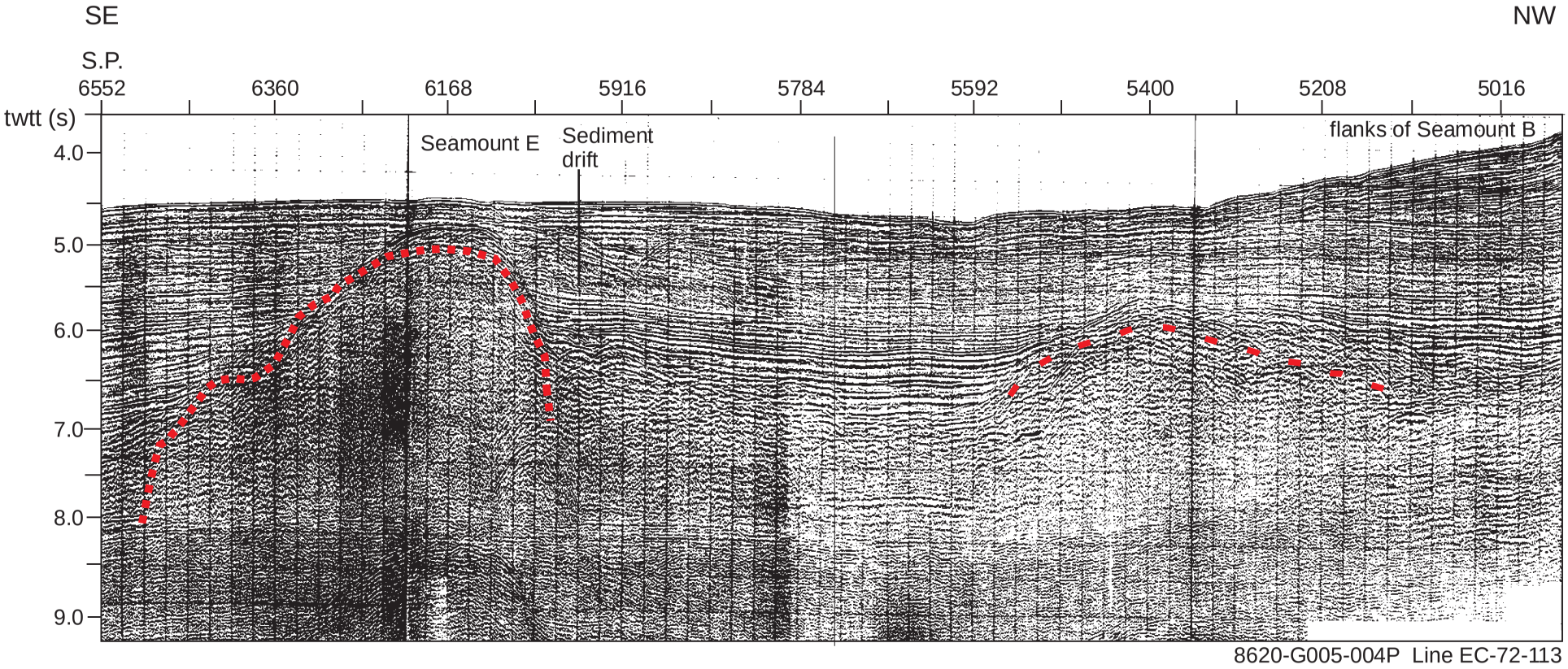

Fig. 13. Seismic reflection profile showing buried seamount E and flanks of seamount B.

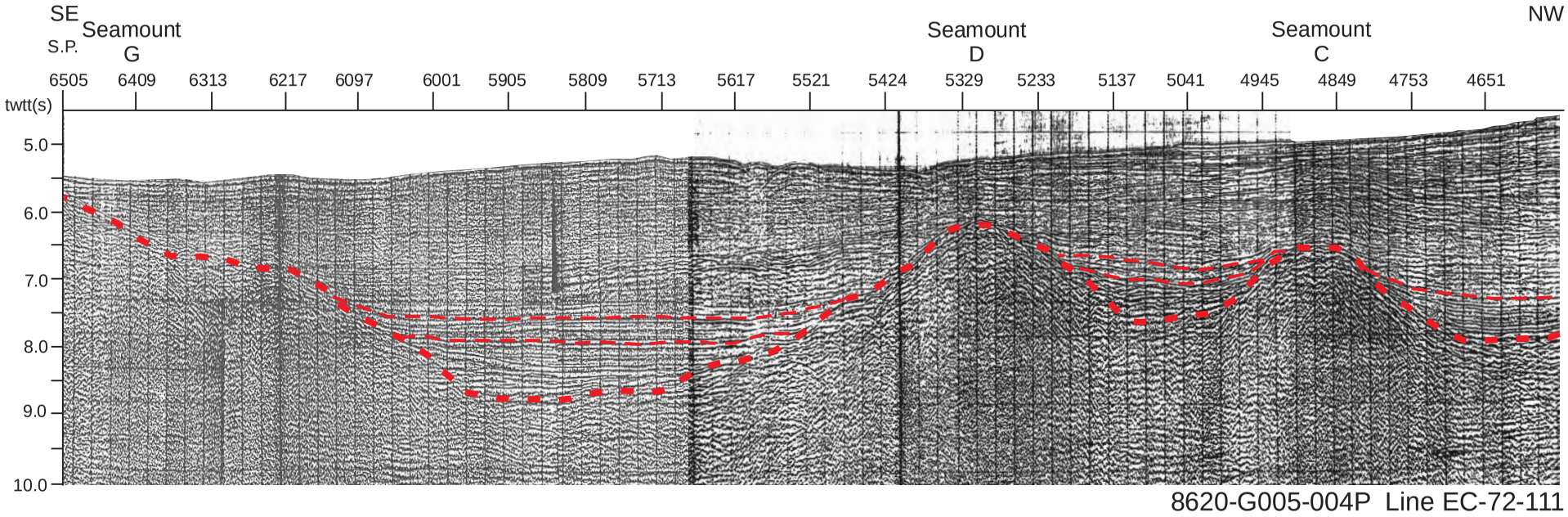

Fig. 14. Seismic reflection profile showing buried seamounts C and D and flanks of large seamount G.

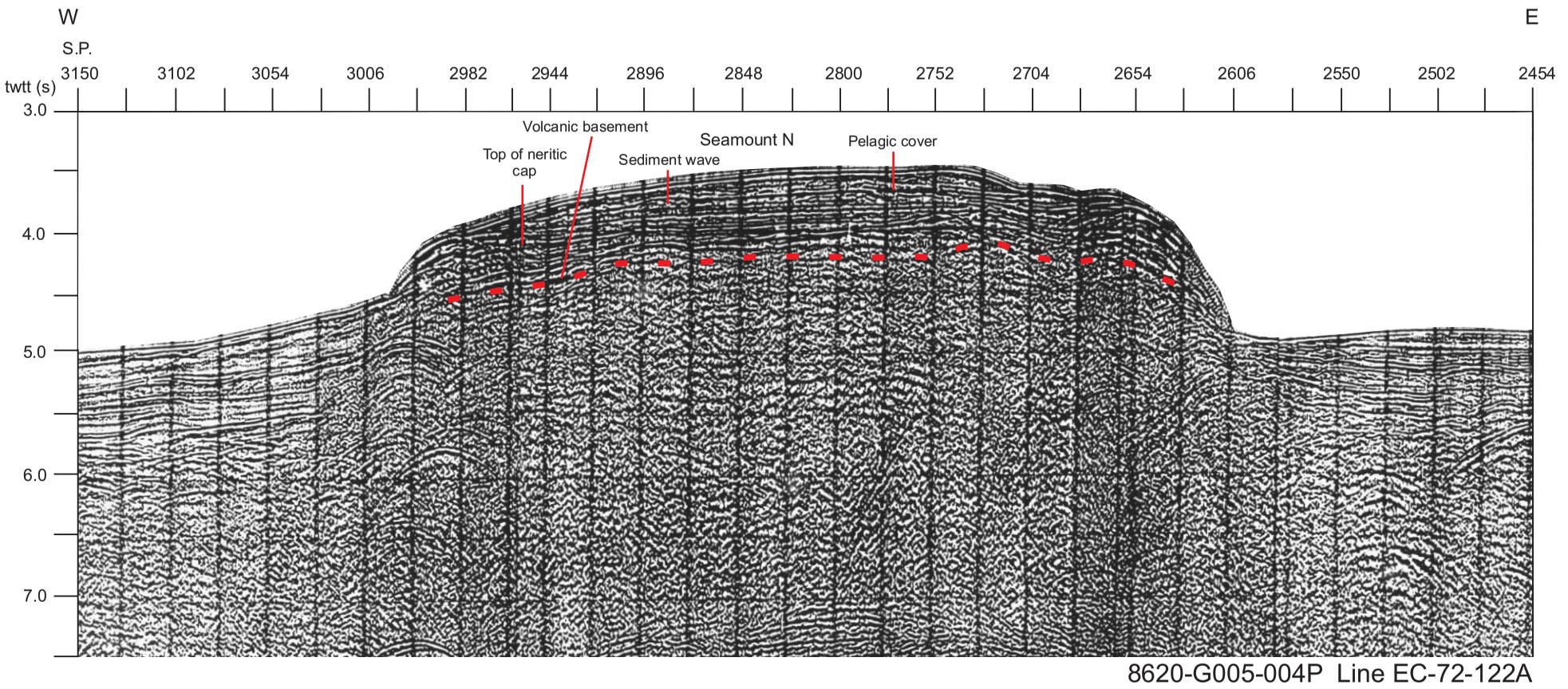

Fig. 15. Seismic reflection profile across seamount N north of the J-Anomaly Ridge.

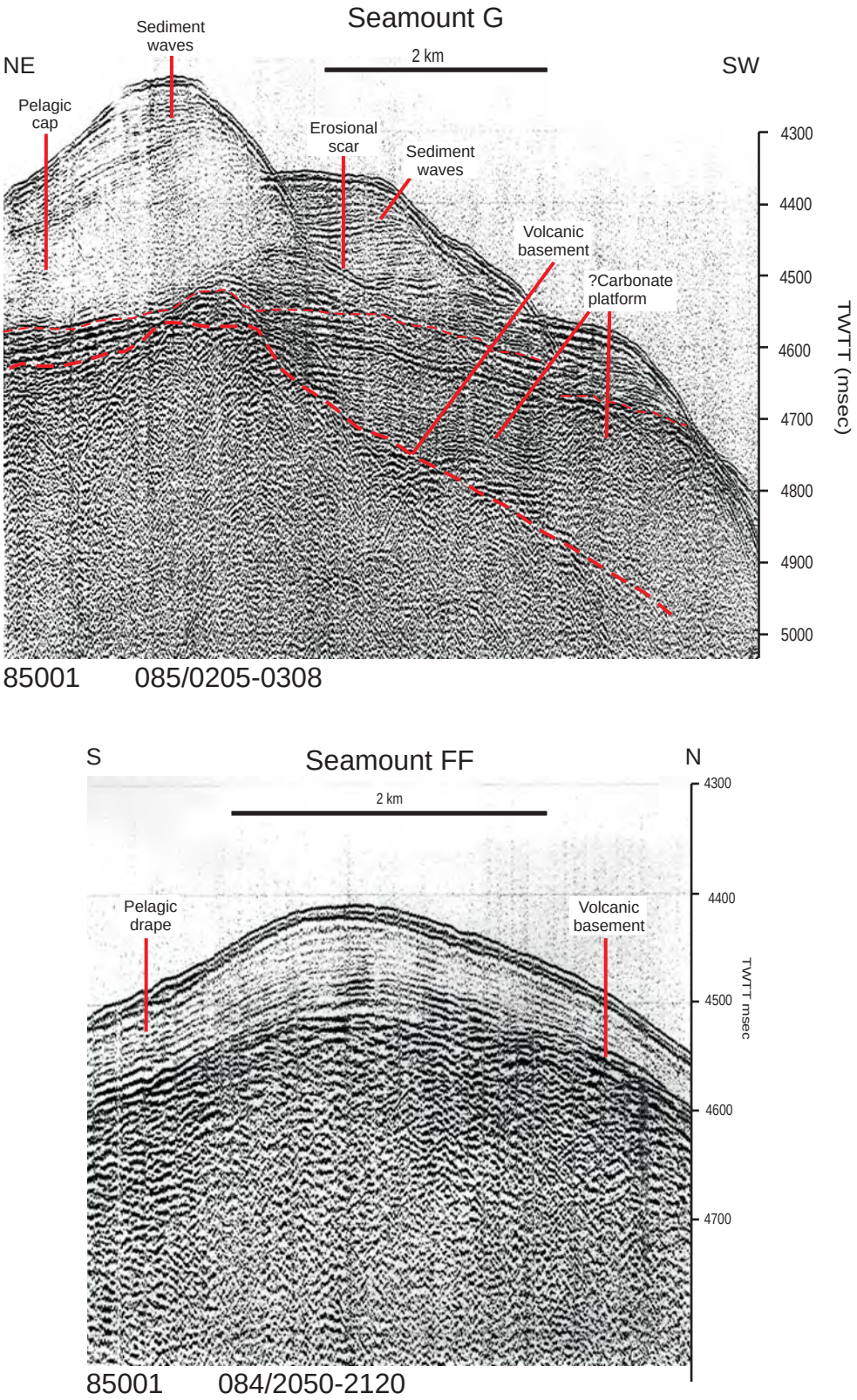

Fig. 16. Single-channel airgun seismic reflection profiles across seamounts G (above) and FF (below).

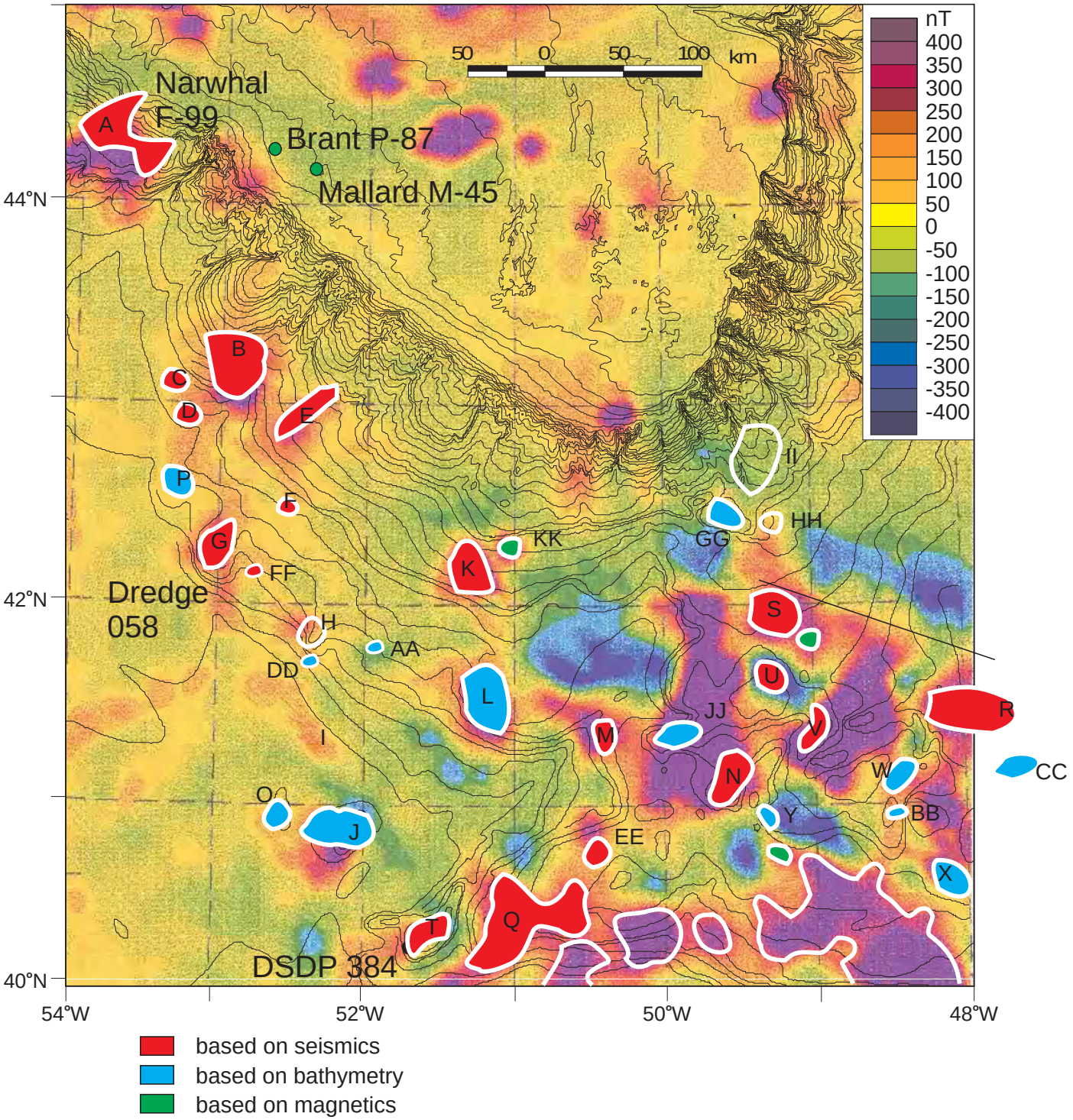

Fig. 17. Map showing locations of seamounts based on (a) seismic reflection profiles; (b) based on bathymetric expression and (c) based on magnetic data. Uncoloured features are either previously misidentified or completely speculative features. See Table 2 for details of sources.

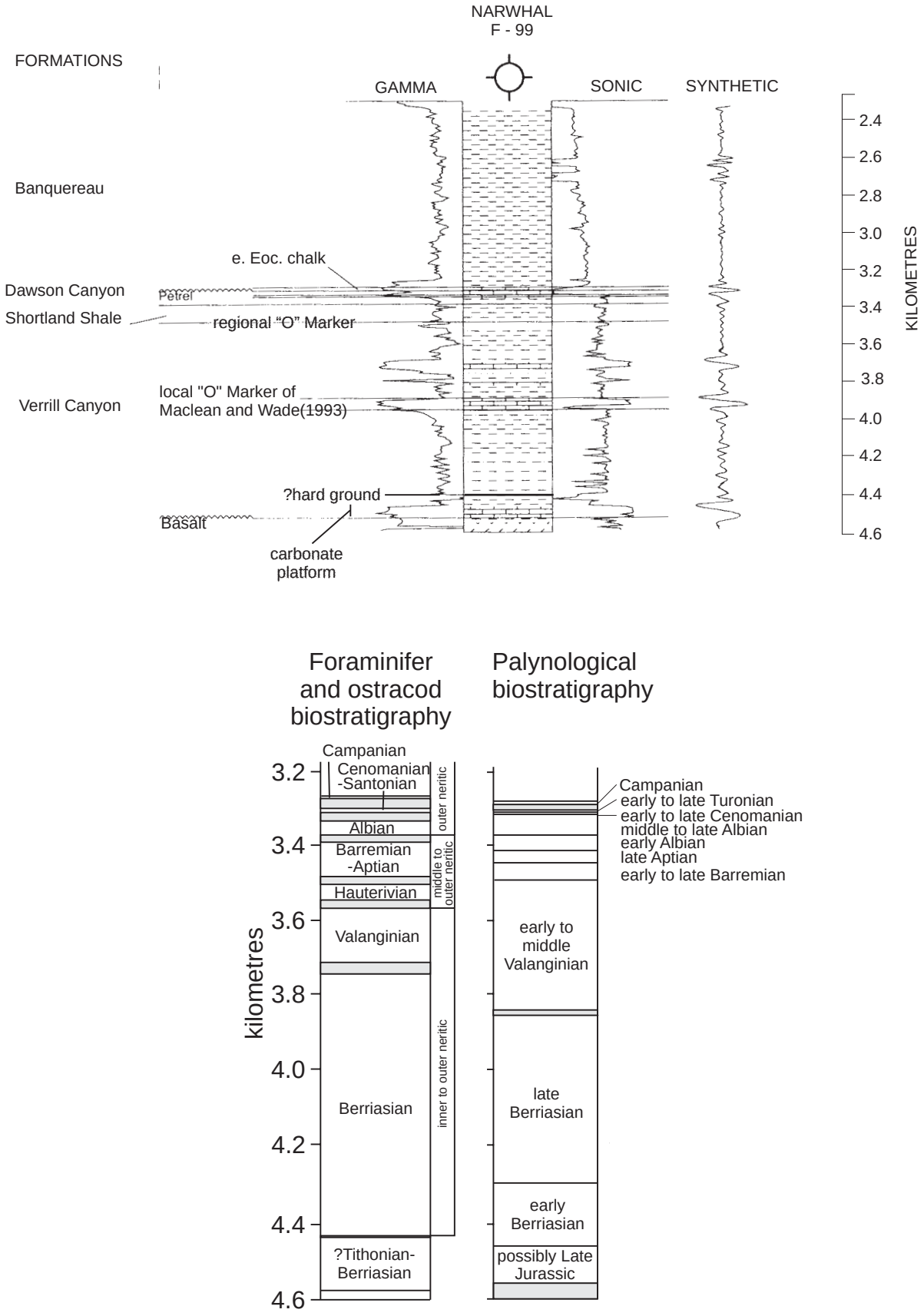

Fig. 18. (a) Well log of the Narwhal F-99 with summary biostratigraphy (from MacLean and Wade 1993). (b) Mesozoic biostratigraphic picks in the Narwhal F-99 well (after Bujak-Davies 1987 and Ascoli 1989).

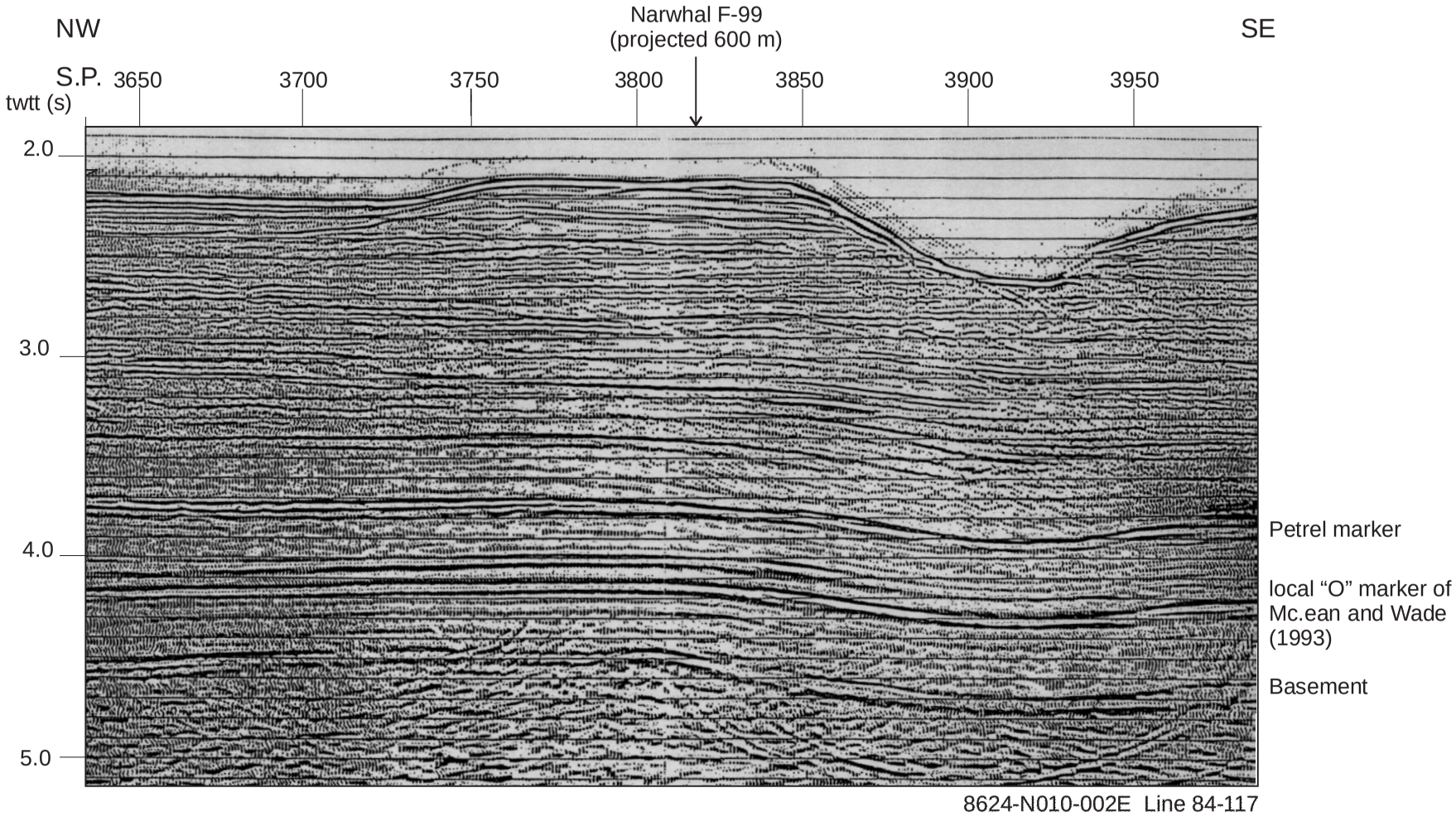

Fig. 19. Seismic reflection profile near the Narwhal F-99 well, showing basement, the local O-marker of MacLean and Wade (1993) and the Petrel marker.

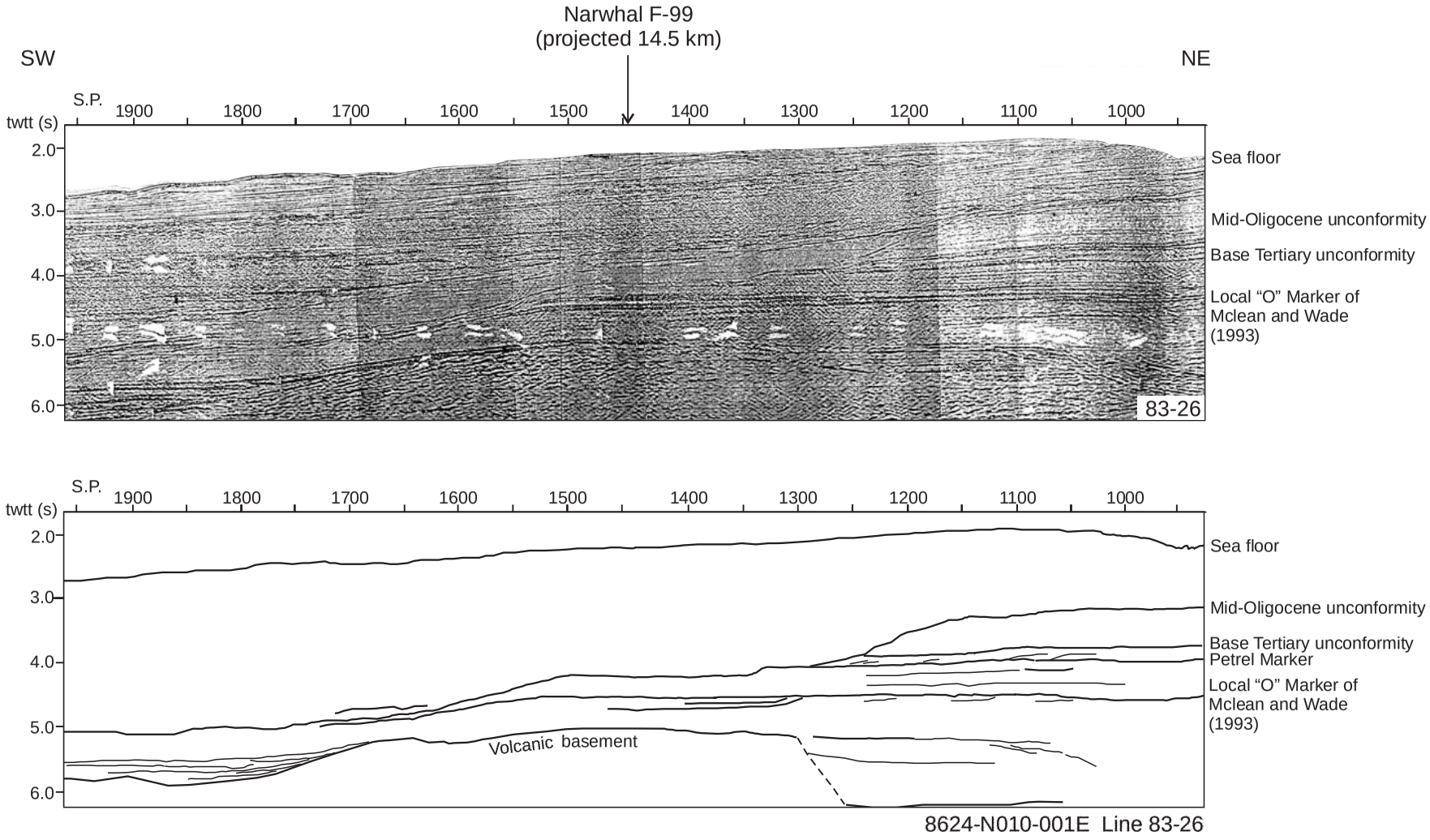

Fig. 20. Seismic reflection profile showing seismic stratigraphy near the Narwhal well.

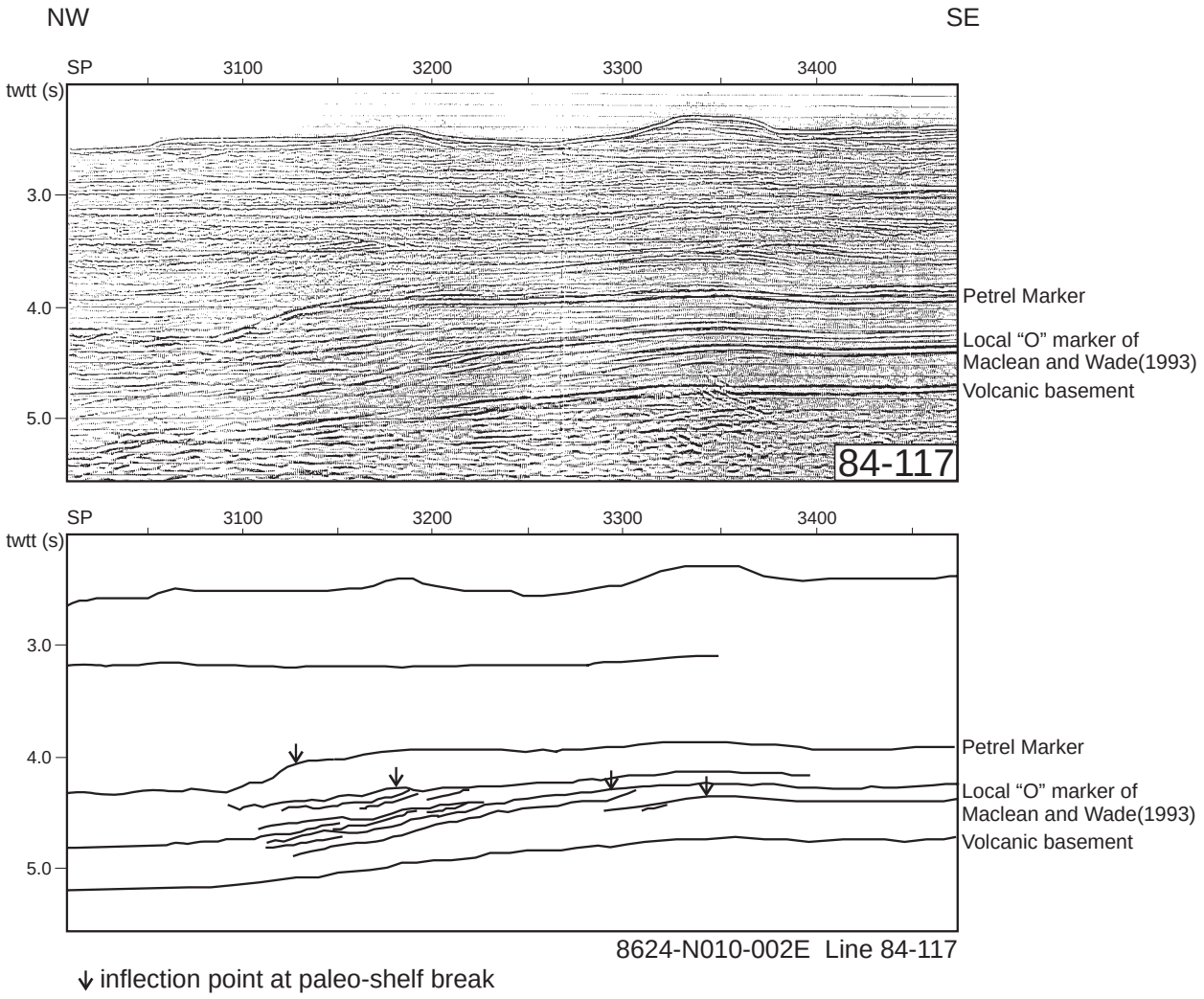

Fig. 21. Seismic reflection profile showing seismic stratigraphy near the Narwhal well.

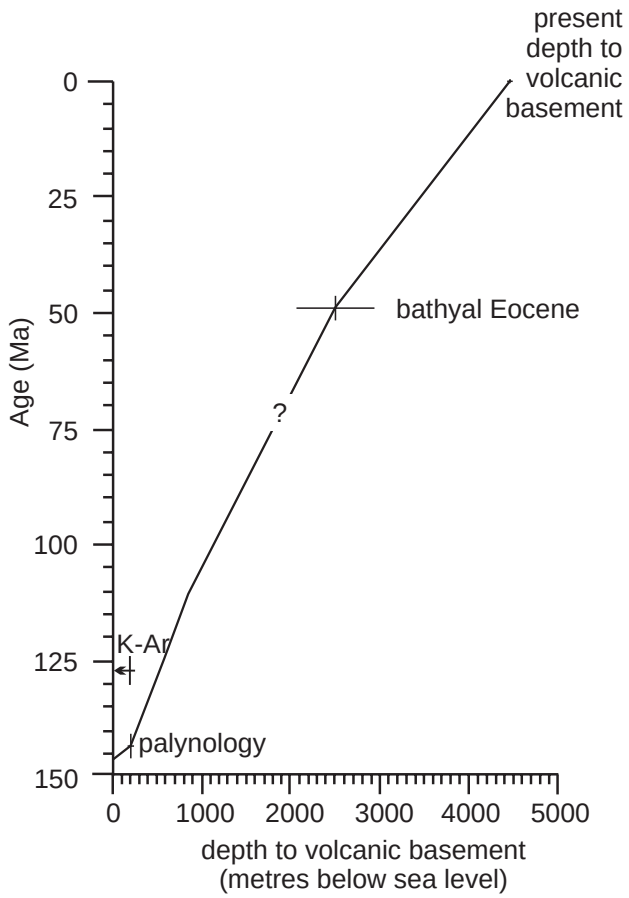

Fig. 22. Age-depth plot for the Narwhal well.

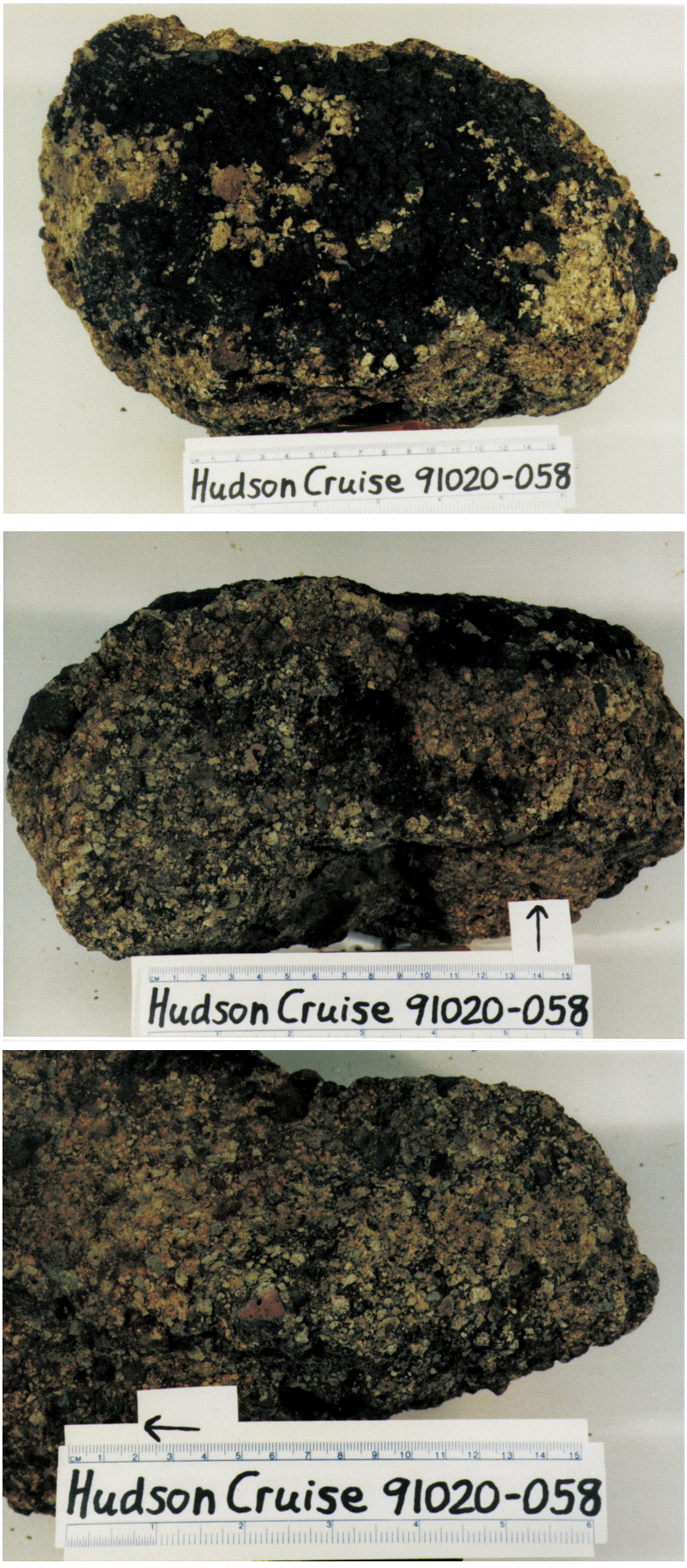

Fig. 23. Photograph of conglomerate from dredge sample 91020-058.

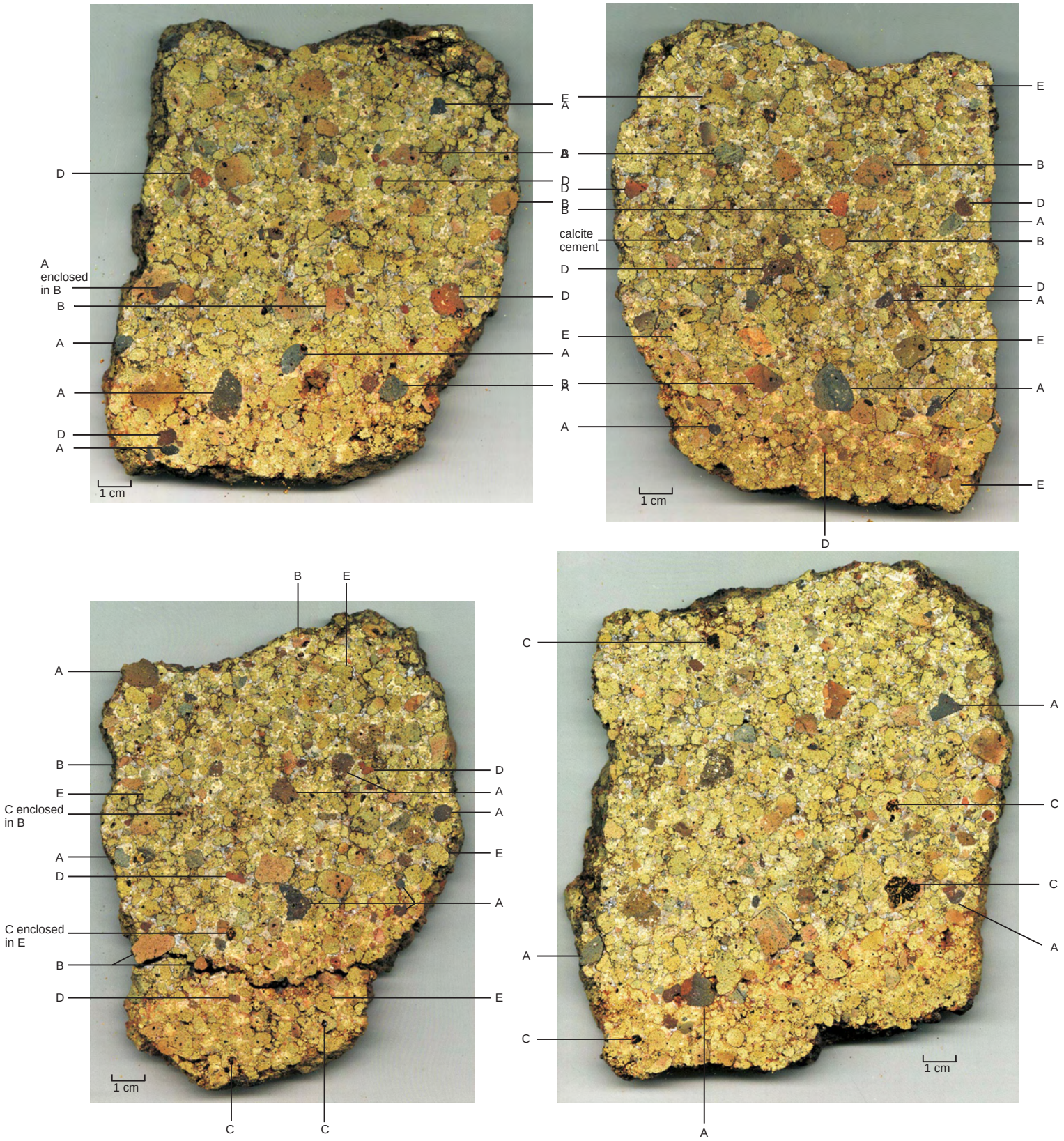

Fig. 24. Photographs of slabbed samples of conglomerate from dredge 91020-058. Clast types A to E are described in text.

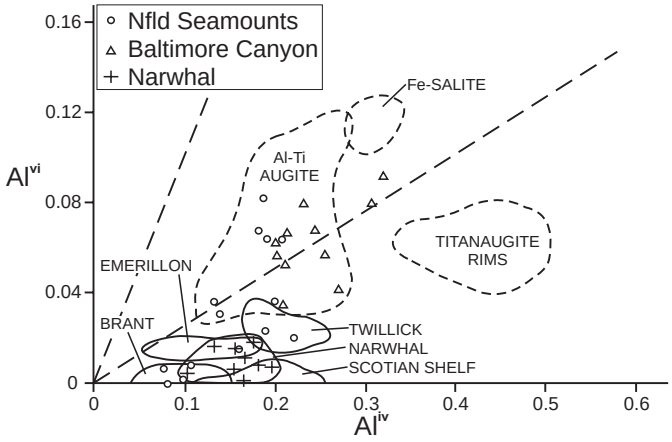

Fig. 25. Graph of Al^{vi} vs. Al^{iv} for pyroxenes from basalts from the Narwhal well and other early Cretaceous igneous rocks on the eastern North American margin. Straight dashed lines are limits of field for high-pressure pyroxenes (after Wass, 1979); dashed fields are for the New England Seamounts (after Pe-Piper and Jansa, 1988).

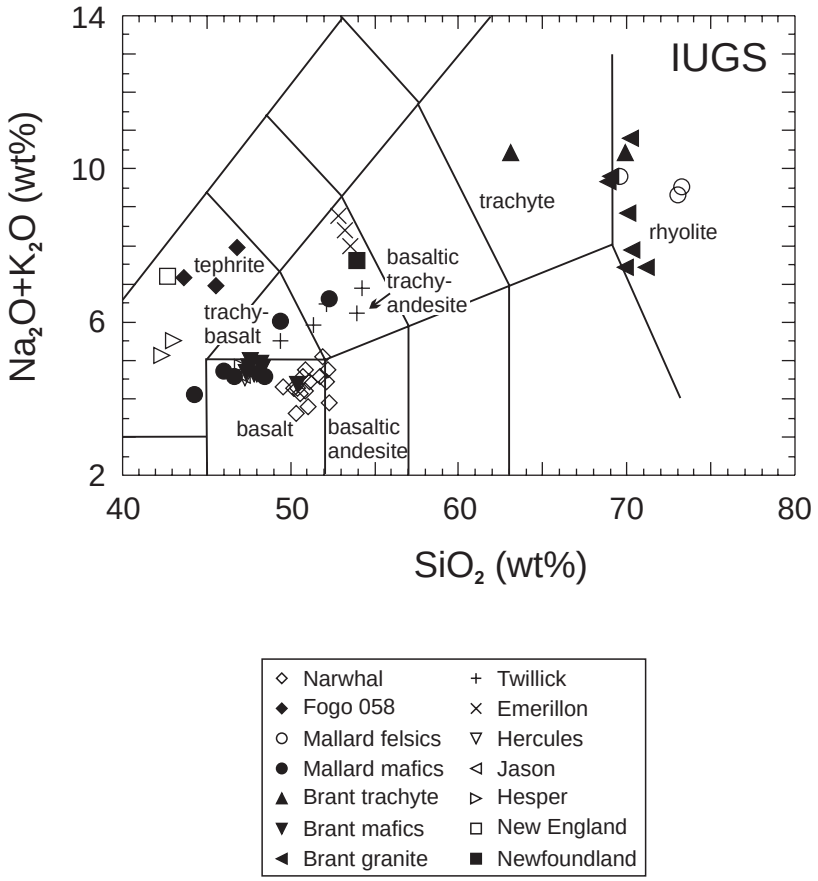

Fig. 26. IUGS nomenclature for selected Cretaceous igneous rocks on the southeastern Canadian margin.

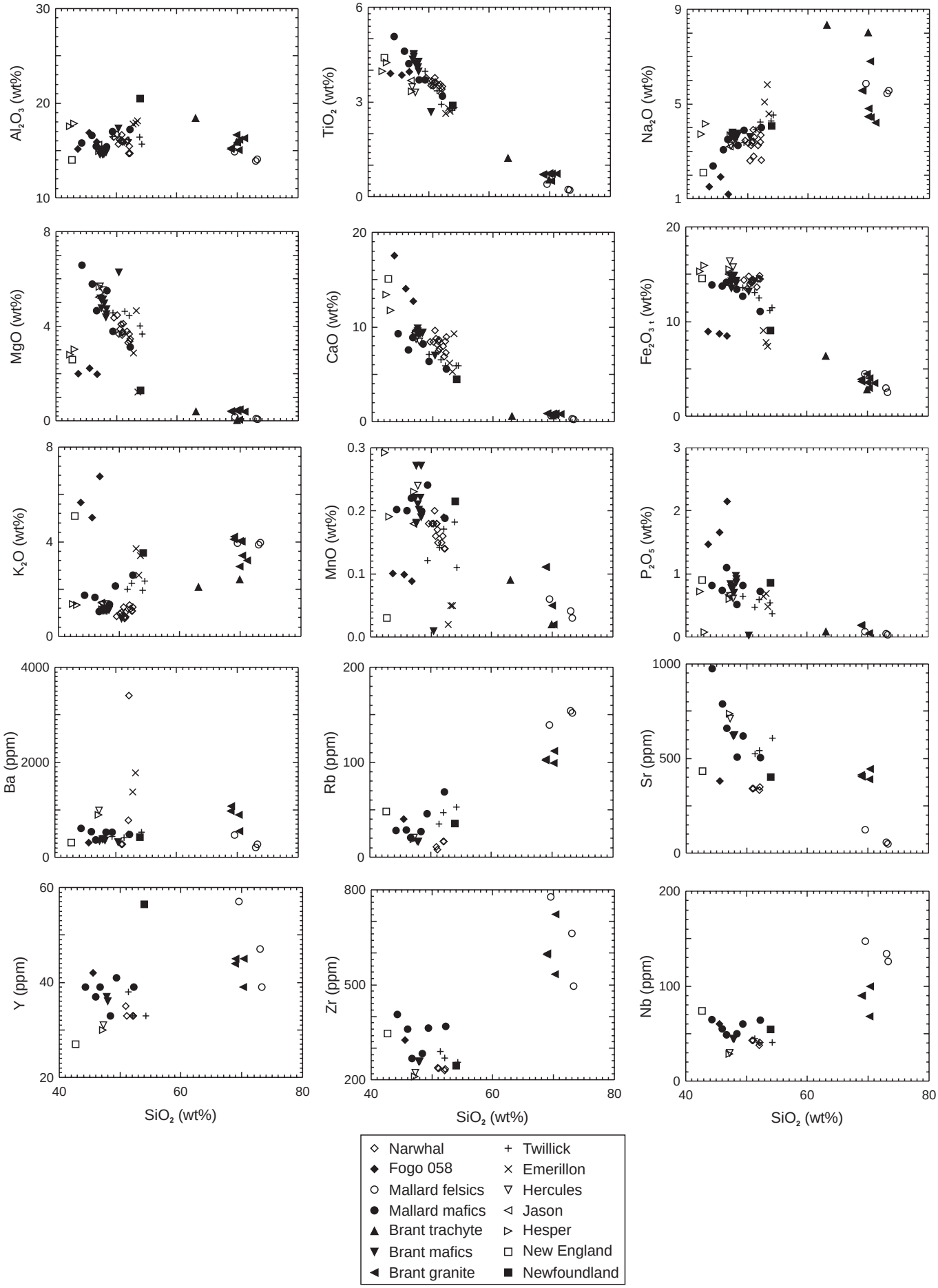

Fig. 27. Plots of elemental abundance vs. SiO_2 (Harker diagrams) for selected Cretaceous igneous rocks on the southeastern Canadian margin.

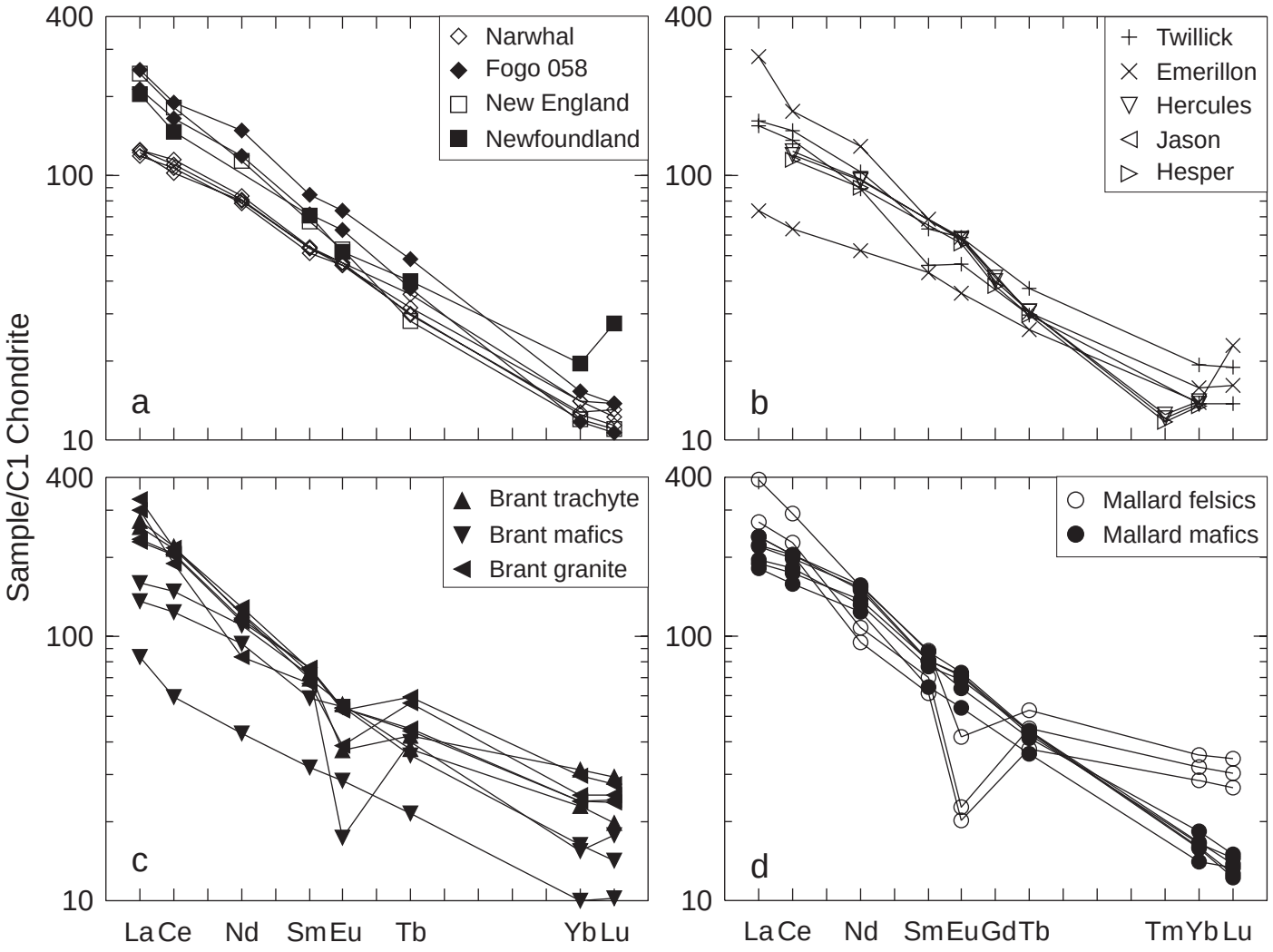

Fig. 28. Rare Earth element abundances normalised to C1 chondrite for selected Cretaceous igneous rocks on the southeastern Canadian margin.

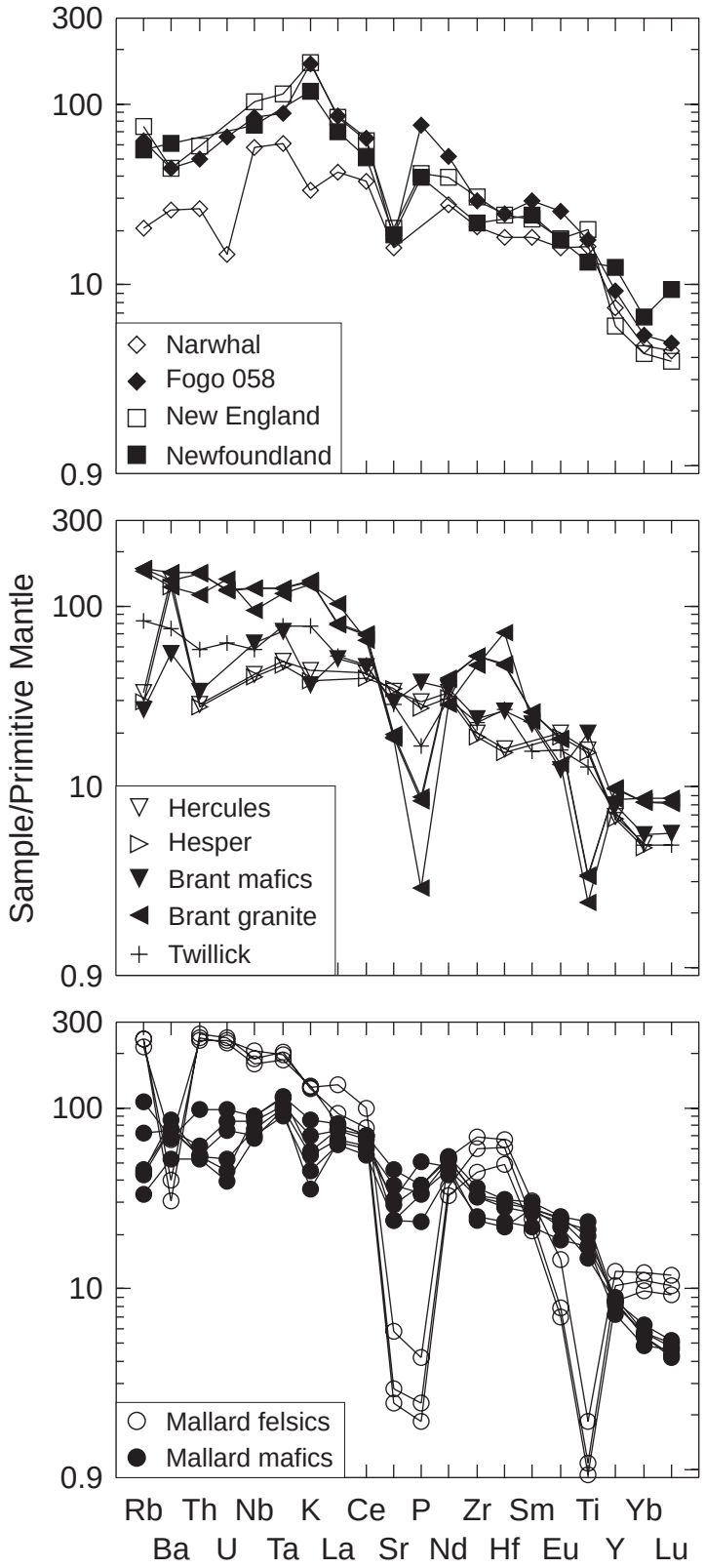

Fig. 29. Trace element abundances normalised to primitive mantle (Sun and McDonough 1989) for selected Cretaceous igneous rocks on the southeastern Canadian margin.

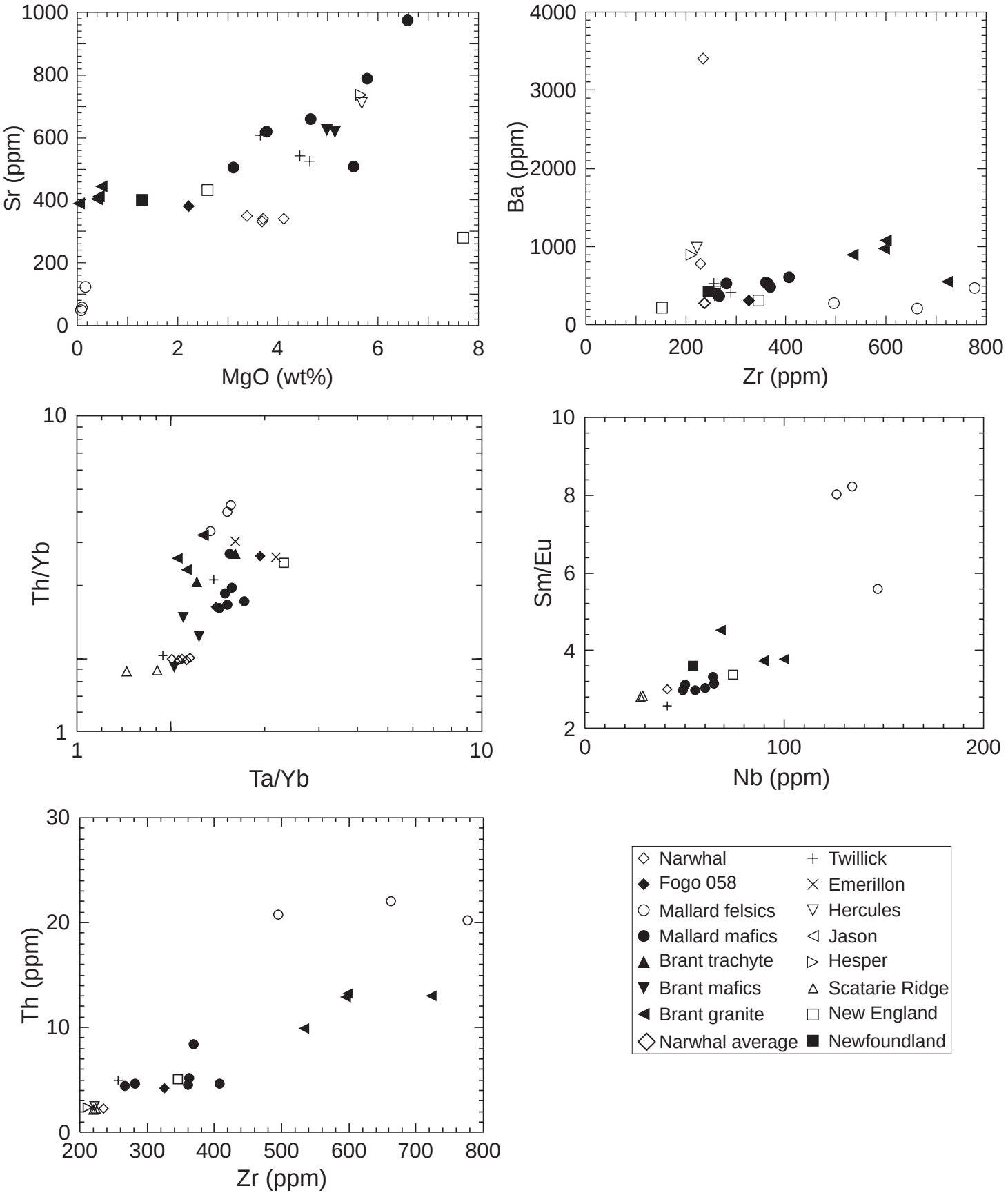

Fig. 30. Selected binary element plots for Cretaceous igneous rocks on the southeastern Canadian margin.

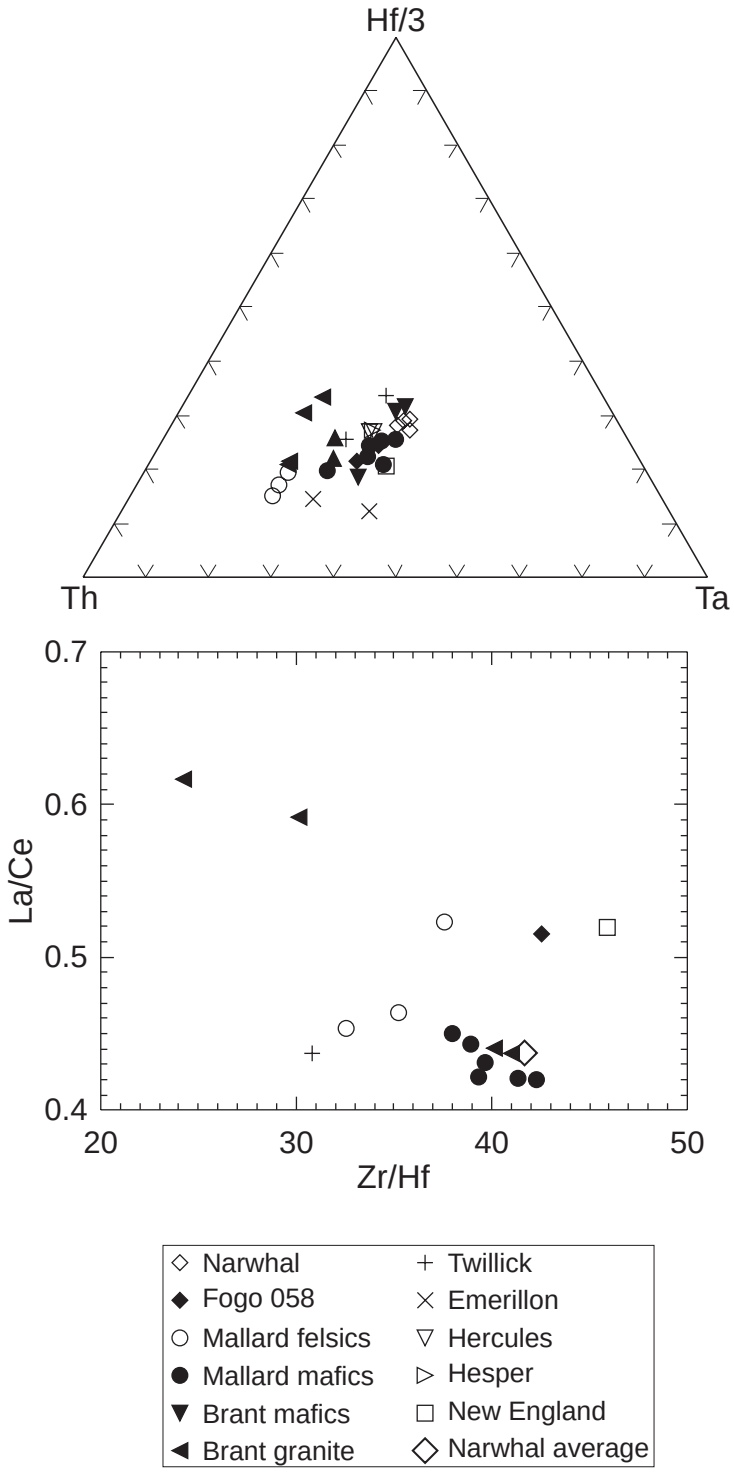

Fig. 31. Comparison of Narwhal trace elements Hf, Zr, Th, Ta, La and Ce with other east coast offshore volcanic rocks.

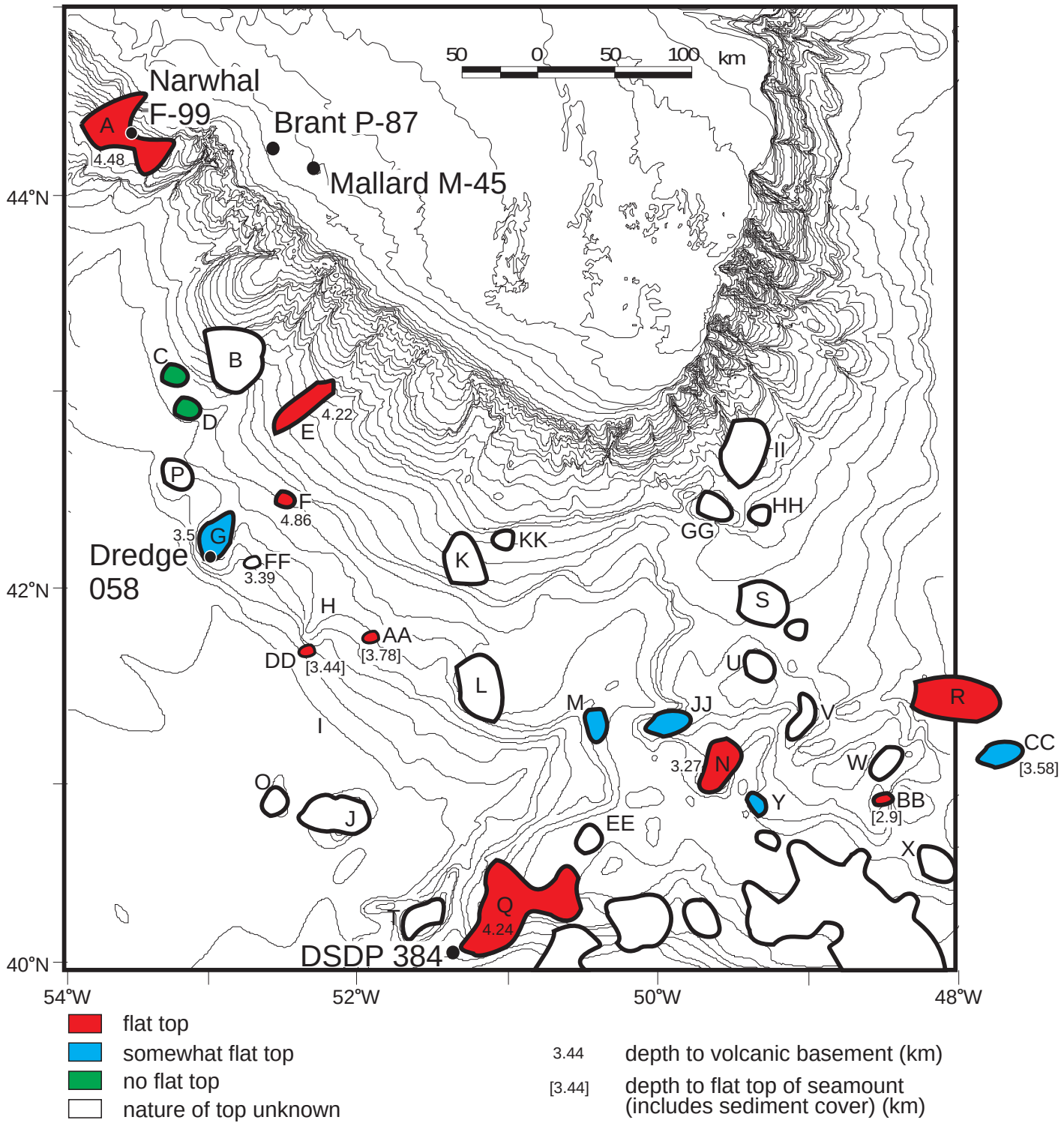

Fig. 32. Type of flat top and depths to flat tops of seamounts.

Table 1: Geochronology of igneous rocks on eastern Canadian continental margin

Sample location	Depth	Type of date	Material dated	Analyzed age (Ma)	Reference Laboratory if new date
Seamounts					
Dredge 058					
F1	dredge 058	K/Ar	whole rock	85.4±2.2	Krueger Geochronological Laboratory
F1	dredge 058	$^{40}Ar/^{39}Ar$	kaersutite	130.3±1.3	Geological Survey of Canada
Narwhal	4570-4580	K/Ar	whole rock	127±6	Krueger Geochronological Laboratory
Grand Banks					
Brant (basalt)	lower unit	K/Ar	whole rock	135±6	Amoco et al (1974)
Mallard (basalt)	8670-8680	K/Ar	whole rock	128±3	Pe-Piper et al (1994)
	9750-9830	K/Ar	whole rock	127±4	Pe-Piper et al (1994)
Mallard (fels.)	8510-8670	K/Ar	whole rock	133±3	Pe-Piper et al (1994)
	9110-9530	K/Ar	whole rock	134±3	Pe-Piper et al (1994)
Emerillon	2990	K/Ar	whole rock	96.4±3.8	Jansa and Pe-Piper (1986)
Twillick		K/Ar	whole rock	117±5	Amoco et al (1974)
Scotian Shelf					
Hercules	713.23	K/Ar	whole rock	119±5	Jansa and Pe-Piper (1985)
	713.23	K/Ar	whole rock	102.9±2.6	Jansa and Pe-Piper (1985)
Hesper	2743.2	K/Ar	whole rock	112±5	Jansa and Pe-Piper (1985)
	2743.2	K/Ar	whole rock	125.9±3.2	Jansa and Pe-Piper (1985)
Scatarie Bank	diabase sill	K/Ar	whole rock	127±15	Wanless et al (1979)

Table 2. Inventory of seamounts

Seamount code	Descriptive name	Flat top (seismic) s	Flat top (bathy) kmbsl	Flat or not	Seismic expression	Bathymetric	Magnetic expression	Source
A	Narwhal	4.6-5.1	4.478	flat	Y	N	Y	Narwhal F-99 well, industry seismic
B					Y	N	Y	Fig. 13
C		6.50		not	Y	N	N	Fig 14
D		6.10		not	Y	N	N	Fig 14
E		4.80	4.22	flat	Y	N	Y	Fig.13
F		6.00	4.86	flat	Y	N	N	Fig 11
G	Dredge 58	4.60	3.5	partly	Y	Y	Y	Figs. 11, 14, 16
H'						Y	Y	absent, relocated at DD
I							?Y	minor magnetic feature
J			3.5			Y	Y	Hughes Clarke (1988) Hudson 87008
K						Y	Y	industry seismic
L		<5.5	3.4		Y	Y	Y	Sullivan (1978), Hudson 75009
M		5.60	3.4	partly	Y	Y	Y	Sullivan (1978), Hudson 75009
N		4.10	3.27	flat	Y	Y	Y	Fig. 15, Tucholke et al. (1986)
O						Y	?Y	Hughes Clarke (1988) Hudson 87008
P						Y	?Y	Hughes Clarke (1988)
Q		??6.1		flat?	Y	Y	Y	Sullivan (1978), Hudson 72021
R		5.30		flat?	Y	?Y	?Y	Sullivan (1978), Hudson 75009
S					Y	Y	Y	Vema 2702
T	DSDP 384	4240 m (drill) = 5.65 s	4115 m (drill to reef top)					Sullivan (1978), Hudson 72021; Tucholke, Vogt et al. (1979)
U		3.35				Y	Y	Tucholke et al. (1986)
V						Y	Y	Tucholke et al. (1986)
W								ETOPO5, near magnetic high.
X								ETOPO5, near magnetic high.
Y			3.1	partly				ETOPO5, near magnetic high.
Z					Y	Y		Hudson 98039
AA			3.78	flat		Y	?N	bathymetric lines
BB			2.9	flat				bathymetric lines
CC			3.58	partly				bathymetric lines
DD			3.44					bathymetric lines
EE		6.05 or 6.5						Vema 2702
FF		4.52	3.39	partly				Hudson 85001, Fig. 16
GG								Basin Atlas bathymetry, magnetics
HH							no	high on seismic basement
II							no	high on seismic basement
JJ								Basin Atlas bathymetry, magnetics
KK								based solely on magnetics

Table 3: Representative electron microprobe chemical analyses of glass fragments (dark colored) and K-feldspars from dredge 91020-058

GLASS

Sample	Fogo1	Fogo1	Fogo1	D-4-B
An. No	5	6*	1	1
SiO_2	50.59	42.41	50.68	46.17
TiO_2	1.31	2.46	3.16	2.40
Al_2O_3	17.17	14.39	18.10	14.81
FeO_t	8.37	8.08	7.03	7.30
MgO	3.53	3.48	3.43	3.50
CaO	2.84	5.53	2.37	4.13
Na_2O	1.30	1.40	1.76	1.31
K_2O	2.98	4.56	2.84	2.79
Cl	0.09	0.41	-	-
P_2O_5	-	2.37	0.42	2.35
Total	88.18	85.09	89.79	84.76

* This chemical analysis of this glass fragment is the closest to the whole rock chemistry of the analysed clasts for all oxides except CaO

Sample	FOGO1						FOGO2		
An. No	1	2	3	4	5	6	7	8	9
SiO_2	65.14	65.17	64.39	64.71	66.73	65.47	66.73	65.58	67.38
Al_2O_3	18.65	18.72	18.32	18.60	18.71	18.87	19.10	18.89	18.82
Na_2O	0.23	0.28	-	-	-	-	-	-	-
K_2O	16.47	16.52	16.39	16.63	14.42	15.13	14.25	14.21	14.40
Total	100.49	100.69	99.10	99.94	99.86	99.47	100.08	98.68	100.6

Sample	FOGOA			FOGOB		FOGOC			
An. No	10	11	12	13	14	15	16	17	18
SiO_2	66.20	66.47	64.91	66.22	67.01	66.81	65.70	66.25	67.04
Al_2O_3	19.13	18.87	18.44	19.43	18.88	18.73	19.22	18.54	18.64
K_2O	14.67	14.53	15.03	13.62	14.54	15.89	13.32	13.82	14.02
Total	100.00	99.87	98.38	99.27	100.43	101.43	98.24	98.61	99.7

Table 4: Representative electron microprobe chemical analyses of amphiboles from dredge 91020-058

Sample	FOGO1	FOGO2	FOGOA		FOGOB			FOGOC	
An. Po[1]	2	r	1	2	c	i	r	c	r
SiO_2	39.97	38.43	39.89	40.01	39.10	38.96	39.50	39.07	39.25
TiO_2	5.37	5.24	5.31	5.29	5.45	5.19	5.24	5.54	5.70
Al_2O_3	13.42	14.46	13.68	13.52	13.75	13.56	13.56	13.06	14.32
FeO_t	11.72	12.66	12.25	12.79	12.25	12.37	13.00	12.49	11.70
MnO	-	-	-	-	0.19	-	-	-	-
MgO	12.88	11.40	12.85	12.44	12.07	11.92	12.28	12.37	12.57
CaO	11.85	11.53	11.83	12.02	11.56	11.51	11.81	12.00	11.58
Na_2O	2.77	2.46	2.55	2.54	2.47	2.65	2.62	2.80	2.48
K_2O	0.98	0.96	0.98	0.94	0.92	0.90	0.97	0.95	0.89
Total	98.96	95.14	99.34	99.55	97.76	97.06	98.98	98.28	98.49
Atomic Formulae[2]									
Si	5.85	5.74	5.80	5.83	5.79	5.82	5.80	5.80	5.74
Ti	0.59	0.59	0.58	0.58	0.61	0.58	0.58	0.62	0.63
$^{\{4\}}Al$	2.15	2.26	2.20	2.17	2.21	2.18	2.20	2.20	2.26
$^{\{6\}}Al$	0.17	0.29	0.15	0.16	0.19	0.21	0.14	0.09	0.20
^{3+}Fe	0.12	0.21	0.31	0.21	0.26	0.17	0.27	0.06	0.32
^{2+}Fe	1.31	1.38	1.18	1.35	1.25	1.37	1.32	1.49	1.11
Mn	-	-	-	-	0.02	-	-	-	-
Mg	2.81	2.54	2.79	2.70	2.66	2.66	2.69	2.74	2.74
Ca	1.86	1.85	1.84	1.88	1.83	1.84	1.86	1.91	1.81
Na	0.79	0.71	0.72	0.72	0.71	0.77	0.75	0.81	0.70
K	0.18	0.18	0.18	0.18	0.17	0.17	0.18	0.18	0.17

[1]: Po: position of the analysis: r=rim; c=core; i=between core and rim
[2]: The atomic formulae have been calculated according to the method described by Stout (1972) and Robinson et al. (1982), and we report the 13 total cation values

Table 4 (Continued)

Sample	FOGOC			
An. Po	c	r	c	r
SiO_2	39.11	39.06	38.76	39.50
TiO_2	5.75	5.80	6.05	5.95
Al_2O_3	13.74	13.53	13.76	13.95
FeO_t	12.37	12.48	11.14	11.25
MnO	0.20	0.23	-	-
MgO	12.21	12.21	12.80	12.97
CaO	11.63	11.68	11.82	11.65
Na_2O	2.56	2.57	2.58	2.68
K_2O	0.89	0.91	0.85	0.87
Total	98.46	98.47	97.76	98.82
Atomic Formulae				
Si	5.76	5.76	5.73	5.76
Ti	0.64	0.643	0.67	0.65
$^{\{}Al^{\}}$	2.24	2.24	2.27	2.24
$^{\{}Al^{\}}$	0.14	0.11	0.13	0.16
^{3+}Fe	0.28	0.26	0.15	0.22
^{2+}Fe	1.25	1.28	1.22	1.15
Mn	0.03	0.03	-	-
Mg	2.68	2.68	2.82	2.82
Ca	1.83	1.85	1.87	1.82
Na	0.73	0.73	0.74	0.76
K	0.17	0.17	0.16	0.16

Table 5: Representative electron microprobe analysis of Fe-Ti oxides from dredge 91020-058

Sample	FOGO1
An. No	2
SiO_2	0.29
TiO_2	14.70
Al_2O_3	5.80
FeO_t	67.82
MgO	5.72
Cr_2O_3	0.32
Total	94.65

Table 6: Electron microprobe chemical analyses of secondary* minerals from dredge 91020-058

Sample	FOGO1				FOGO1				FOGOC	
An. No	1	2	3	4	3	4	5	11	12	22
SiO_2	50.58	49.83	48.52	51.27	53.56	53.06	51.16	51.25	48.97	53.22
TiO_2	0.35	0.53	0.64	0.31	-	-	-	-	-	-
Al_2O_3	18.12	20.54	19.02	18.62	18.80	19.00	18.02	19.25	19.30	19.85
FeO_t	8.16	6.51	9.43	7.56	7.95	8.27	7.83	8.14	9.08	8.85
MgO	3.56	3.48	3.26	3.30	4.00	4.10	3.94	3.38	3.76	4.23
CaO	2.91	3.63	2.65	0.45	2.14	2.36	2.07	2.71	2.62	0.73
Na_2O	1.75	0.90	1.15	0.99	1.22	1.04	1.12	1.31	1.76	1.59
K_2O	3.40	2.78	4.16	2.29	2.79	3.01	2.84	3.61	3.86	3.15
Cl	0.11	0.09	-	0.18	-	-	-	-	-	-
P_2O_5	-	0.96	-	-	-	-	-	-	-	-
Total	88.94	89.25	88.83	84.61	90.46	90.84	86.98	89.65	89.35	91.62

* Most of these minerals seem to be products of alteration of glass and some of them rim amygdules

Table 6: (Continued)

Sample	FOGOC	FOGO1	FOGO2	FOGO1	FOGOA(B)		FOGO2	FOGOA	FOGOC
An. No	23	8	15	6	19	20	12	16	19
SiO_2	53.52	44.71	47.79	47.21	46.87	44.65	61.65	67.53	65.81
TiO_2	-	-	-	-	-	-	-	-	-
Al_2O_3	21.50	15.74	16.30	16.94	19.46	15.94	2.99	2.45	1.48
FeO_t	7.59	8.48	11.06	8.51	8.23	7.13	-	-	-
MgO	4.31	3.49	3.33	3.61	3.20	3.18	3.91	4.12	3.94
CaO	1.06	2.54	0.40	2.41	1.58	2.28	5.39	5.65	5.93
Na_2O	1.71	0.97	0.85	1.02	1.69	2.17	9.05	7.59	9.72
K_2O	2.68	3.21	2.35	3.04	3.00	2.62	0.81	0.81	0.87
Cl	-	0.12	0.18	-	-	-	0.32	0.24	0.18
P_2O_5	-	-	-	-	-	-	-	-	-
Total	92.37	79.26	82.26	83.74	84.03	77.97	84.12	88.39	87.93

Table 7: Representative electron microprobe chemical analyses of plagioclase from Narwhal F-99 well

Sample	4580A								
An.Po[1]	ph1c	ph1r	ph2c	ph2r	ph3c	ph3r	gr	gr	gr
SiO_2	47.85	49.49	50.19	49.08	47.72	47.92	54.97	58.60	55.25
TiO_2	0.07	0.10	0.05	0.06	0.05	0.06	0.21	0.15	0.14
Al_2O_3	31.05	29.42	31.26	30.71	32.29	32.09	26.73	24.66	26.74
FeO_t	0.80	0.86	0.82	0.73	0.71	0.84	1.02	0.68	0.97
MgO	0.12	0.10	0.11	0.13	0.10	0.09	0.08	0.02	0.12
CaO	16.83	15.47	17.29	15.74	16.57	16.23	10.45	7.45	10.69
Na_2O	2.59	3.15	2.52	2.76	2.17	2.29	5.65	6.68	5.88
K_2O	0.02	0.09	-	0.01	-	0.04	0.46	0.93	0.43
Total	99.32	98.67	102.24	99.21	99.62	99.56	99.55	99.17	100.21
An	78.13	72.71	79.13	75.87	80.84	79.48	49.24	36.09	48.94
Ab	21.76	26.79	20.90	24.07	19.16	20.29	48.18	58.55	48.72
Or	0.11	0.50	-	0.06	-	0.23	2.58	5.36	2.34
Name[2]	Bt	Bt	Bt	Bt	Bt	Bt	As	As	As

[1]: ph=phenocryst; gr=groundmass; c=core; r=rim
[2]: Bt=bytownite; As=andesine; Lb=labradorite

Table 7: (Continued)

Sample	4580B					
An.Po	ph1c	ph1r	ph2c	ph2r	gr	gr
SiO_2	48.19	47.76	47.77	48.27	53.96	53.90
TiO_2	0.07	0.05	0.06	0.06	0.43	0.14
Al_2O_3	30.59	30.77	32.19	32.28	26.99	28.11
FeO_t	0.78	0.82	0.78	0.85	1.63	0.96
MgO	0.10	0.10	0.12	0.09	0.26	0.09
CaO	16.51	16.61	16.74	16.76	11.40	11.92
Na_2O	2.46	2.35	2.25	2.27	4.93	4.81
K_2O	0.02	0.02	-	0.01	0.40	0.39
Total	98.72	98.49	99.90	100.59	99.99	100.32
An	78.67	79.53	80.44	80.27	54.81	56.52
Ab	21.21	20.36	19.56	19.67	42.90	41.28
Or	0.11	0.11	-	0.06	2.29	2.20
Name	Bt	Bt	Bt	Bt	Lb	Lb

Table 7: (Continued)

Sample	4580C								
Anal. Po	ph1c	ph1r	ph2c	ph2r	ph3c	ph3r	gr	gr	gr
SiO_2	48.75	51.66	47.72	48.66	47.92	48.39	52.77	52.54	55.44
TiO_2	0.05	0.09	0.03	0.06	0.06	0.07	0.14	0.14	0.16
Al_2O_3	30.97	28.42	31.90	30.90	31.84	32.02	27.72	27.89	27.00
FeO_t	0.80	0.98	0.71	0.78	0.79	0.86	1.14	1.15	0.88
MgO	0.12	0.11	0.11	0.12	0.10	0.09	0.10	0.09	0.08
CaO	16.43	13.57	17.02	16.27	16.86	16.70	12.50	12.91	11.13
Na_2O	2.81	4.11	2.27	2.52	2.20	2.19	4.64	4.51	5.53
K_2O	0.04	0.20	-	0.01	0.03	-	0.31	0.25	0.35
Total	99.97	99.14	99.46	99.32	99.80	100.32	99.30	99.57	100.56
An	76.20	63.87	80.56	78.06	80.76	80.82	58.78	60.42	51.64
Ab	23.58	35.01	19.44	21.88	19.07	19.18	39.48	38.19	46.43
Or	0.22	1.12	-	0.06	0.17	-	1.74	1.39	1.93
Name	Bt	Lb	Bt	Bt	Bt	Bt	Lb	Lb	Lb

Table 8: Representative electron microprobe chemical analyses of clinopyroxene from Narwhal F-99 well

Sample	4580-4585								
An.No	1C[1]	2C	3C	1A	2A	3A	1B	2B	3B
SiO_2	48.84	49.00	51.39	49.50	49.88	49.80	49.43	48.67	48.50
TiO_2	1.68	1.46	1.19	1.38	1.29	1.51	1.77	2.20	1.81
Al_2O_3	4.48	4.09	2.53	3.70	3.44	3.97	3.87	4.73	4.34
FeO_t	7.28	7.28	7.75	7.32	6.95	7.41	8.05	8.65	8.19
MnO	0.11	0.11	0.13	0.09	0.11	0.10	0.16	0.14	0.13
MgO	14.92	14.96	16.13	15.16	15.36	15.11	14.95	14.27	14.45
CaO	22.03	22.29	20.96	22.29	21.63	22.11	22.08	22.12	21.96
Na_2O	0.39	0.30	0.34	0.37	0.27	0.36	0.32	0.45	0.42
Cr_2O_3	0.48	0.37	0.10	0.31	0.35	0.29	0.24	0.27	0.24
Total	100.01	99.96	100.61	100.12	9.28	100.68	100.87	101.50	100.04
Atomic Formulae on the basis of 6 Oxygens									
Si	1.82	1.83	1.90	1.84	1.87	1.84	1.83	1.80	1.82
Ti	0.05	0.04	0.03	0.04	0.04	0.04	0.05	0.06	0.05
Al	0.20	0.18	0.11	0.16	0.15	0.17	0.17	0.21	0.19
Fe	0.23	0.23	0.24	0.23	0.22	0.23	0.25	0.27	0.26
Mn	<0.01	<0.01	<0.01	<0.01	<0.01	<0.01	0.01	<0.01	<0.01
Mg	0.82	0.83	0.89	0.84	0.86	0.83	0.83	0.79	0.81
ca	0.88	0.89	0.83	0.89	0.87	0.88	0.88	0.88	0.88
Na	0.03	0.02	0.02	0.03	0.02	0.03	0.02	0.03	0.03

[1]: A, B, C refer to different basaltic chips from the same well interval

Table 9. Representative whole rock chemical analyses from Dredge 058 and the Narwhal F-99 well

Sample No	Dredge 058, Seamount G			Narwhal F-99 well						
	F1[1]	F2	F3	4550A[2]	4550B	4515A	4515B	4570A	4570B	4540A
Major elements (wt%) (XRF:F1, F2, F3; all others by electron microprobe)										
SiO_2	41.3	42.2	38.9	51.09	52.1	51.03	52.27	49.56	50.75	50.91
TiO_2	3.49	3.56	3.48	3.63	3.27	3.76	3.49	3.76	3.51	3.61
Al_2O_3	15.31	14.33	13.48	15.91	14.73	15.97	14.72	16.45	16.01	16.65
Fe_2O_{3t}	7.87	7.67	7.98	14.47	14.55	14.22	14.53	14.37	14.18	14.11
MnO	0.09	0.08	0.09	0.15	0.19	0.17	0.14	0.18	0.16	0.18
MgO	2.02	1.78	1.78	4.11	3.68	3.77	3.47	4.36	4.09	3.71
CaO	12.73	11.45	15.63	7.67	8.47	8.68	8.96	8.45	8.13	7.47
Na_2O	1.74	1.08	1.34	3.59	3.39	2.78	2.63	3.45	3.37	3.92
K_2O	4.55	6.09	5.04	0.84	1.07	1.02	1.25	0.85	1.23	0.84
P_2O_5	1.5	1.94	1.31	n.d.	n.d.	n.d.	n.d.	n.d.	n.d.	n.d.
L.O.I	11.2	11.5	14	n.d.	n.d.	n.d.	n.d.	n.d.	n.d.	n.d.
Total	101.8	101.68	103.03	100.01	99.99	99.98	100	99.99	100.01	99.99
Trace elements by XRF (ppm)										
Ba	308	n.d.	n.d.	275	781	n.d.	n.d.	n.d.	n.d.	272
Rb	40	n.d.	n.d.	8	17	n.d.	n.d.	n.d.	n.d.	11
Sr	382	n.d.	n.d.	340	333	n.d.	n.d.	n.d.	n.d.	341
Y	42	n.d.	n.d.	33	33	n.d.	n.d.	n.d.	n.d.	35
Zr	325	n.d.	n.d.	237	229	n.d.	n.d.	n.d.	n.d.	238
Nb	60	n.d.	n.d.	43	38	n.d.	n.d.	n.d.	n.d.	43
Th	0	n.d.	n.d.	0	0	n.d.	n.d.	n.d.	n.d.	0
P	0	n.d.	n.d.	26	46	n.d.	n.d.	n.d.	n.d.	26
Ga	15	n.d.	n.d.	22	23	n.d.	n.d.	n.d.	n.d.	22
Zn	541	n.d.	n.d.	125	121	n.d.	n.d.	n.d.	n.d.	123
Cu	21	n.d.	n.d.	43	50	n.d.	n.d.	n.d.	n.d.	38
Ni	30	n.d.	n.d.	38	41	n.d.	n.d.	n.d.	n.d.	34
V	175	n.d.	n.d.	342	321	n.d.	n.d.	n.d.	n.d.	343
Cr	14	n.d.	n.d.	37	36	n.d.	n.d.	n.d.	n.d.	25
REE and selected trace elements by INAA (ppm)										
La	59.22	50.09	n.d.	n.d.	n.d.	n.d.	n.d.	n.d.	n.d.	n.d.
Ce	115	101	n.d.	n.d.	n.d.	n.d.	n.d.	n.d.	n.d.	n.d.
Nd	69.07	55.28	n.d.	n.d.	n.d.	n.d.	n.d.	n.d.	n.d.	n.d.
Sm	12.97	10.91	n.d.	n.d.	n.d.	n.d.	n.d.	n.d.	n.d.	n.d.
Eu	4.28	3.6	n.d.	n.d.	n.d.	n.d.	n.d.	n.d.	n.d.	n.d.
Tb	1.8	1.4	n.d.	n.d.	n.d.	n.d.	n.d.	n.d.	n.d.	n.d.
Yb	2.6	1.99	n.d.	n.d.	n.d.	n.d.	n.d.	n.d.	n.d.	n.d.
Lu	0.35	0.27	n.d.	n.d.	n.d.	n.d.	n.d.	n.d.	n.d.	n.d.
Co	30.52	26.06	n.d.	n.d.	n.d.	n.d.	n.d.	n.d.	n.d.	n.d.
Hf	7.64	7.44	n.d.	n.d.	n.d.	n.d.	n.d.	n.d.	n.d.	n.d.
Sc	13.8	10.01	n.d.	n.d.	n.d.	n.d.	n.d.	n.d.	n.d.	n.d.
Ta	3.65	3.86	n.d.	n.d.	n.d.	n.d.	n.d.	n.d.	n.d.	n.d.
Th	4.22	5.26	n.d.	n.d.	n.d.	n.d.	n.d.	n.d.	n.d.	n.d.
U	1.39	0.73	n.d.	n.d.	n.d.	n.d.	n.d.	n.d.	n.d.	n.d.

Sample No	Narwhal F-99 well						
	4540B	4575A	4575B	4535A	4535B	4585A	4585B
Major elements (wt%) (by electron microprobe)							
SiO_2	52.21	50.17	51.66	50.91	51.88	50.58	50.37
TiO_2	3.41	3.67	3.51	3.55	3.56	3.66	3.53
Al_2O_3	15.44	16.7	15.93	16.08	16.08	16.15	15.65
Fe_2O_{3t}	14.86	13.46	13.64	14.34	14.49	13.99	14.81
MnO	0.14	0.18	0.15	0.18	0.16	0.2	0.18
MgO	3.38	4.48	3.78	3.63	3.3	3.88	3.68
CaO	7.27	8.41	7.96	8.51	6.88	8.78	9.63
Na_2O	3.69	3.33	3.25	3.44	3.93	3.25	2.6
K_2O	1.08	0.96	1.32	0.77	1.18	0.89	1.02
P_2O_5	n.d.	n.d.	n.d.	n.d.	n.d.	n.d.	n.d.
L.O.I	n.d.	n.d.	n.d.	n.d.	n.d.	n.d.	n.d.
Total	99.99	100.01	99.83	99.99	100.01	99.98	99.99
Trace elements by XRF (ppm)							
Ba	3405	n.d.	n.d.	n.d.	n.d.	n.d.	n.d.
Rb	17	n.d.	n.d.	n.d.	n.d.	n.d.	n.d.
Sr	350	n.d.	n.d.	n.d.	n.d.	n.d.	n.d.
Y	33	n.d.	n.d.	n.d.	n.d.	n.d.	n.d.
Zr	234	n.d.	n.d.	n.d.	n.d.	n.d.	n.d.
Nb	41	n.d.	n.d.	n.d.	n.d.	n.d.	n.d.
Th	0	n.d.	n.d.	n.d.	n.d.	n.d.	n.d.
Pb	61	n.d.	n.d.	n.d.	n.d.	n.d.	n.d.
Ga	22	n.d.	n.d.	n.d.	n.d.	n.d.	n.d.
Zn	121	n.d.	n.d.	n.d.	n.d.	n.d.	n.d.
Cu	43	n.d.	n.d.	n.d.	n.d.	n.d.	n.d.
Ni	37	n.d.	n.d.	n.d.	n.d.	n.d.	n.d.
V	320	n.d.	n.d.	n.d.	n.d.	n.d.	n.d.
Cr	44	n.d.	n.d.	n.d.	n.d.	n.d.	n.d.
REE and selected trace elements by INAA (ppm)							
La	n.d.	28.93	28.09	29.63	29.71	n.d.	n.d.
Ce	n.d.	62.47	65.61	67.68	70.13	n.d.	n.d.
Nd	n.d.	37.37	36.54	37.79	38.97	n.d.	n.d.
Sm	n.d.	8.15	7.8	8.12	8.23	n.d.	n.d.
Eu	n.d.	2.67	2.65	2.72	2.73	n.d.	n.d.
Tb	n.d.	1.12	1.18	1.11	1.33	n.d.	n.d.
Yb	n.d.	2.13	2.38	2.18	2.4	n.d.	n.d.
Lu	n.d.	0.29	0.31	0.33	0.35	n.d.	n.d.
Co	n.d.	43.1	37.79	41.1	41.71	n.d.	n.d.
Hf	n.d.	5.72	5.62	5.5	5.7	n.d.	n.d.
Sc	n.d.	24.36	23.5	24.58	22.85	n.d.	n.d.
Ta	n.d.	2.46	2.4	2.32	2.69	n.d.	n.d.
Th	n.d.	2.14	2.36	2.15	2.36	n.d.	n.d.
U	n.d.	n.d.	0.3	n.d.	0.32	n.d.	n.d.

n.d.: not determined; [1] Samples F1,F2, F3: are different clasts from dredge 058;
[2] A indicates coarse grained cuttings, whereas B indicates fine grained cuttings

Table 10. Sm/Nd isotopic data for early Cretaceous igneous rocks from the eastern Canadian continental margin[1]

Sample	Lab[4]	SiO_2 wt %	Sm ppm	Nd ppm	$^{147}Sm/^{144}Nd$ measured	$^{143}Nd/^{144}Nd$ measured	Age (Ga)	ϵ_{Nd}[2] initial	T_{DM}[2] (Ga)
Dredge 91020-058from seamount G									
F1ba[3]	GSC	43	12.89	66.09	0.1180	0.51277	0.135	3.91	0.51
F2ba	UCSC	46.8	25.56	127.26	0.1240	0.51269	0.135	2.27	0.66
Narwhal F-99 well									
4535ba	GSC	50.9	8.12	36.14	0.1359	0.51282	0.135	4.68	0.51
4575ba	UCSC	50.3	17.73	74.68	0.1465	0.51274	0.135	2.86	0.76
Brant P-87 well (Pe-Piper et al. 1994)									
10280tr	UCSC	~63.1	21.81	118.59	0.1135	0.51276	0.135	3.81	0.5
11050gr	RL	70	9.63	48.25	n.d.	0.51274		3.30	
11060gr	RL	71	11.39	57.57	n.d.	0.51268		2.14	
11070gr	UCSC	68.4	11.36	58.30	0.1203	0.51282	0.135	4.87	0.44
11080gr	UCSC	~69	10.58	53.23	0.1227	0.51281	0.135	4.63	0.47
11630F[5]ba	GSC	~47.6	10.58	49.08	0.1304	0.51286	0.135	5.47	0.42
11710S[5]ba	GSC	~47.6	10.60	48.97	0.1309	0.51286	0.135	5.37	0.43
Mallard M-45 well (Pe-Piper et al. 1994)									
7770-7830ba	RL	47.1	12.24	57.79	n.d.	0.51271	0.135		
9110ba	RL	~45	9.65	44.85	n.d.	0.51341	0.135		
8310-8740fs	UCSC	~70	25.25	135.04	0.1154	0.51266	0.135	1.83	0.65
8550-8560fs	UCSC	72.9	19.11	102.57	0.1154	0.51260	0.135	0.66	0.74
Scatarie Bank (Jansa et al. 1993)									
73-2-355ba	GSC	~45	8.58	40.23	0.13442	0.51263	0.135	0.96	0.84
Hercules J-15 well (Jansa and Pe-Piper, 1985)									
2570-2590ba	GSC	~47	9.80	48.00	0.1234	0.51265	0.135	1.44	0.72
Hesper I-52 well (Jansa and Pe-Piper, 1985)									
9000ba	GSC	~43	8.77	43.25	0.1226	0.51265	0.135	1.47	0.72
Exxon 133-1 well, Georges Bank (Pe-Piper and Jansa, 1987)									
13440 ba	RL	~47	17.0	84.2	0.1214	0.51287	0.140	5.87	0.37
Scruncheon Seamount, Newfoundland Seamounts (Sullivan and Keen, 1977)									
25/2 ba	RL	61	11.4	65.0	0.1055	0.51279	0.098	4.11	0.42
DSDP Site 382, Nashville Seamount, New England Seamounts (Tucholke and Vogt, 1979)									
25-2-105 ba	RL	~43	8.8	44.6	0.1150	0.51279	0.082	3.82	0.46
DSDP Site 385, Vogel Seamount, New England Seamounts (Tucholke and Vogt, 1979)									
23-1-148 ba	RL	~43	10.3	53.3	0.1162	0.51266	0.91	1.36	0.65

[1]: Analytical methods as in Pe-Piper et al. (1994) for UCSC; in Pe-Piper et al. (1992) for RL.

[2]: These values are calculated at 135 Ma, an age corresponding to the early Cretaceous, although igneous rocks from individual wells and dredge 058 may have a little different ages (see Table 1)

[3]: The two letter abbreviation after each sample number indicates the lithology analysed: ba=basalt; tr=trachyte; gr=granite; fs=felsite

[4]: Laboratories: UCSC = University of California at Santa Cruz, by Z. Palacz, reported in Pe-Piper et al. (1994); GSC = Geological Survey of Canada, Ottawa lab; RL = the late R.St.J. Lambert (personal communication, 1991), using the University of Alberta lab.

[5]: F = float fraction, S = sink fraction in tetrabromoethane.

Table 11. Sr and Pb isotopic data for early Cretaceous igneous rocks from the eastern Canadian continental margin

Locality Depth	Lab	Rock type	Age	File	$^{87}Sr/^{86}Sr_i$	$^{206}Pb/^{204}Pb$	$^{207}Pb/^{204}Pb$	$^{208}Pb/^{204}Pb$
Dredge 058 F2	UCSC	mafic	100	6-215	0.70649	n.d.	n.d.	n.d.
Narwhal 4575A	UCSC	mafic	127	3-609	0.70374	n.d.	n.d.	n.d.
Mallard M-45 well 8310-8340	UCSC	felsic	135	6-217	0.71689	19.725	15.686	39.895
Mallard M-45 well 8550-8560	UCSC	felsic	135	6-218	0.71898	19.592	15.646	39.685
Brant P-87 well 11640	RL	mafic	135	1-649	0.7040	18.752	15.636	38.674
Brant P-87 well 11480	RL	mafic	135	1-654	0.7036	18.609	15.636	38.617
Brant P-87 well 11470	RL	mafic	135	1-655	0.7036	18.538	15.598	38.505
Brant P-87 well 11050	RL	felsic	135	3-620	n.d.	18.569	15.637	38.637
Brant P-87 well 11060	RL	felsic	135	3-618	n.d.	19.278	15.676	39.076
Brant P-87 well 10280	UCSC	felsic	135	3-619	0.70539	19.081	15.605	39.166
Brant P-87 well 11070	UCSC	felsic	135	3-615	0.70546	n.d.	n.d.	n.d.
Brant P-87 well 11080	UCSC	felsic	135	3-617	0.70555	19.083	15.617	39.208
Twillick C-49 well 4230	RL	mafic	117	1-661	0.7044	19.252	15.693	39.312
Twillick C-49 well 4270	RL	mafic	117	1-657	0.7050	20.150	15.798	40.297
Hercules J-15 well 2570-90	RL	mafic	119-103	1-676	0.7035	18.266	15.552	37.880
Hercules J-15 well 2540	RL	mafic	119-103	1-677	0.7054	18.697	15.573	38.106
Hesper P-82 well 9000	RL	mafic	112-126	1-679	0.7051	n.d.	n.d.	n.d.
Scatarie Bank 73-2-355	UCSC	mafic	127		0.70509	n.d.	n.d.	n.d.
Scruncheon Seamount 25/2	RL	mafic	98	1-712	0.7036	19.164	15.565	39.209
Scruncheon Seamount 25/3	RL	mafic	98	1-713	0.7048	19.145	15.554	39.198
Scruncheon Seamount 25/9	RL	mafic	98	1-714	0.7040	20.230	15.609	29.195
Scruncheon Seamount 25/32	RL	mafic	98	1-715	0.7058	18.867	15.626	38.717
Dipper Seamount 30/2	RL	mafic	100	1-716	0.7038	19.588	15.622	39.034
Nashville Smnt DSDP 382 25/2/105	RL	mafic	79-88	1-82	0.7034	20.375	15.668	40.091
Nashville Smnt DSDP 382 25/2/107	RL	mafic	79-88	1-83	0.7037	20.330	15.678	39.667
Vogel Seamount DSDP 385 23/1/148	RL	mafic	91	1-84	0.7041	20.545	15.686	40.082
Vogel Seamount DSDP 385 23/1/97 91	RL	mafic	91	1-85	0.7043	20.416	15.683	39.780
Georges Bank Exxon 133-1 well 13440	RL	mafic	134-140	1-668	0.7033	19.007	15.610	38.519
Georges Bank Exxon 133-1 well 13470	RL	mafic	134-140	1-667	0.7035	19.102	15.553	38.381
Mobil 544-1 Baltimore Canyon 9550-70	RL	mafic	96-103	1-675	0.7058	18.753	15.657	38.831
Mobil 544-1 Baltimore Canyon 10478	RL	mafic	96-103	1-670	0.7037	18.911	15.659	38.951

Abbreviations and codes as in Table 10